UNIVERSIDADE D
COIMBRA

João Miguel Vicente Ventura

MECHANISTIC STUDIES ON THE ENZYMATIC CONJUGATION OF BIOPOLYMERS WITH BIOACTIVE COMPOUNDS

Dissertação no âmbito do Mestrado em Bioquímica orientada pela Doutora Alexandra Teresa Pires Carvalho e pela Senhora Professora Paula Cristina Veríssimo Pires e apresentada ao Departamento de Ciências da Vida.

Julho de 2021

FACULDADE DE CIÊNCIAS E TECNOLOGIA
UNIVERSIDADE D COIMBRA

CENTER FOR NEUROSCIENCE AND CELL BIOLOGY
UNIVERSITY OF COIMBRA PORTUGAL

Mechanistic studies on the enzymatic conjugation of polyesters with bioactive compounds

João Miguel Vicente Ventura
Master's degree in Biochemistry
Department of Life Sciences
Faculty of Science and Technology
University of Coimbra

Supervisors:
Alexandra Carvalho, PhD, Rational Protein Engineering ,Group – CNC
Paula Veríssimo, PhD, Department of Life Sciences

Index

Abstract

Infection by multi-resistant bacteria is rising in likelihood and is often life threatening. One of the proposed solutions is the introduction of antimicrobial peptides as antibiotics. However, these compounds suffer from a short half-life and can display cytotoxic effects, particularly severe haemolytic activity. Polymeric modification of their moieties allows an increase in their effectiveness, altering their pharmacokinetics and pharmacodynamics properties.

In this work we evaluated the conjugation effectiveness with polycaprolactone as a modification to improve the AMPs, specifically polymyxin B and polyphemusin I. Polymyxin B is one of the last line antibiotics and polyphemusin I, - while not in medical use, has been shown to be effective against a broad spectrum of microorganisms.

We intended to 1) verify the impact in their mechanism of action, particularly in the interaction between the cell membranes and the conjugates and 2) the micelles remain stable in water. We have performed classical Molecular Dynamics simulations and analysed their structure and dynamics in water.

In this work, we succeeded in creating a stable micelle with PCL and polymyxin B and prepared a membrane model to test the micelle.

Sumário

Infeções por bactérias multirresistentes são cada vez mais prováveis e são frequentemente um risco de vida. Uma das potenciais soluções para combater o aparecimento de é a introdução de péptidos antimicrobianos como antibióticos. Contudo, estes compostos têm limitações, como tempo de semivida demasiado curto ou efeitos secundários demasiado perigosos,

Uma das soluções para os tornar mais eficazes é a sua modificação com polímeros, para alterar a sua farmacocinética e farmacodinâmica. A polimixina B é um antibiótico de última linha e a polifemusina I mesmo não tendo uso medico, demonstrou em laboratório ser eficaz contra uma vasta gama de microrganismos

Este trabalho teve por objetivo avaliar a eficácia da conjugação dos péptidos antimicrobianos polimixina B e polifemusina I com o polímero policaprolactona como potencial modificação para melhorar os seus efeitos.

Procurou verificar que 1) não há impacto no mecanismo de ação, nomeadamente a interação entre membranas e os conjugados e 2) verificar que as micelas se mantem estáveis em água. Foram realizadas simulações de dinâmica molecular clássica e analisada a estrutura e dinâmica dos compostos em água.

Neste trabalho, conseguimos com sucesso criar uma micela estável com PCL e polimixina B e criar uma membrane modelo para testar a membrana.

Abbreviations

AMBER- Assisted Model Building with Energy Refinement

AMP- Antimicrobial Peptides

CalB- *Candida antartica* Lipase B

CHARMM-GUI- Chemical Harvard Molecular Mechanics graphical user interface

CMS- colistin methanesulfaonate

DFT- Density Functional Theory

DNA- Desoxiribonucleic Acid

LPS - Lipopolysaccharides

MD- Molecular Dynamics

MIC- Minimum Inhibitory Concentration

MM- Molecular Mechanics

NAMD- Nanoscale Molecular Dynamics

QM- Quantum Mechanics

QM/MM- Quantum Mechanics/Molecular Mechanics

PCL- Polycaprolactone

PDB- Protein Data Bank

PEG- Polyethylene glycol

PMB- Polymyxin B

RNA- Ribonucleic Acid

SASA- Solvent Accessible Surface Area

vdW- van der Waals

VMD- Visual Molecular Dynamics

Figure Index

Equation Index

Objectives

Our aim was to perform a *in silico* study about the conjugation of antimicrobial peptides (AMPs), specifically Polymyxin B and Polyphemusin I, with a polycaprolactone (PCL, a biopolymer), to improve their therapeutic potential.

To achieve this, we proposed to perform: (i) Establish molecular models for Polymyxin B, Polyphemusin I, and Polycaprolactone; (ii) Simulate (with Molecular Mechanics) the behaviour of the conjugated AMP with PCL in water to guaranty the formation of stable micelles; (iii) Simulate (with Molecular Mechanics) the interaction with a membrane-model to verify if the mechanism of action is not compromised by modification; and last (iv) Characterize the formation of the conjugate though Quantum mechanics/Molecular mechanics simulation.

Introduction

Antimicrobial Peptides

Antimicrobial peptides (AMPs) are part of the innate defence systems of many organisms (Lei et al., 2019). In microorganisms they evolved as a strategy to overcome competition, while in multicellular organisms they are part of the non specific defence system against infections.

The most common mechanism is the disruption of the membrane stability with the formation of pores that lead to cell lysis (Martin-Serrano, Gómez, Ortega, & Mata, 2019), although some have immunomodulating functions or regulate inflammation (Magana et al., 2020) and some have intracellular targets like DNA, RNA or proteins (Zhu, Liu, & Niu, 2017).

They are classified into two groups: non-ribosomal synthesis, which are produced by enzymes; and ribosomal synthesis which are encoded in genes. The former is most common in bacteria whereas the later is common in all species (Hancock, 2000). Natural AMPs are small peptide sequences - 12 to 50 amino acids - with a broad spectrum of target pathogens (Zhu et al., 2017), and have good water solubility and thermal stability (Lei et al., 2019). About 50% are hydrophobic and mainly composed of basic amino acids (lysine, arginine and histidine), which gives them a positive charge, from +2 to +9 (Hancock, 2000).

AMPs are characterized by their secondary structure as α-helix, β-sheet extended and loop (Sandreschi, Piras, Batoni, & Chiellini, 2016; Zhu et al., 2017). The most common are α-helix and β-sheet, with α-helix being the most studied. There are two main types of tertiary structure: an amphipathic two-faced shape where one is apolar and the other positively charged; and a hydrophobic core with two wings of hydrophilic pockets (Hancock, 2000). Often they only obtain the functional structure in contact with the membranes,

having a random structure in free solution (Hancock, 2000). AMPs, rather than acting on specific intracellular targets like conventional antibiotics, disrupt the membrane with electrostatic interactions (Sun et al., 2018). However they have poor stability, salt sensitivity, and toxicity to mammalian cells (Sun et al., 2018).

In this age of antibiotic resistance where all classes of antibiotics have at least one known mechanism of resistance (Sandreschi et al., 2016), there are approximately 25000 yearly deaths in the EU caused by bacterial resistance to antibiotic (Sandreschi et al., 2016).

AMPs are part of the initiative to replace the failing antibiotics. Since these peptides can act both on membrane lipids and internal components, their non-specific mechanism is leaves fewer opportunities for the development of resistance compared to other antibiotics (Javia et al., 2018; Sun et al., 2018). In figure 1 is represented both the mechanisms of antibacterial action of AMPs and various mechanisms of antibiotic resistance of bacteria

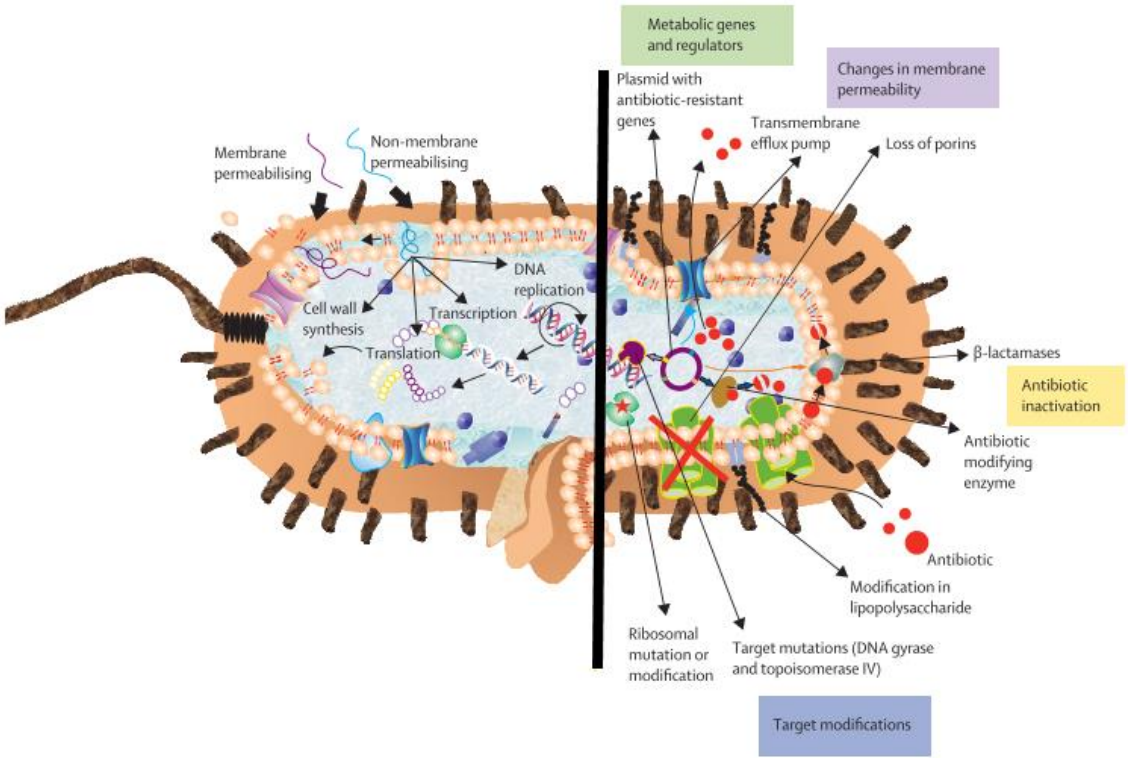

Figure 1- A representation of a Gram-negative bacteria cell, illustrating the mechanisms of action of antimicrobial peptides (on the left of the line) and mechanisms of resistance against antibiotics (right of the line). Adapted from Magana *et al.*, 2020.

However, their use is limited due to cytotoxic side effects. There is a growing interest in designing new AMPs to surpass the limitations of natural AMPs (Martin-Serrano et al., 2019).

Among these are the polymyxins, a group with two antibiotics currently in use (polymyxin B and colistin), cyclic lipodecapeptides which are effective against Gram-negative bacteria. They are non-ribosomal peptides synthesized by a enzyme complex, containing nonstandard amino acids in their composition, with a total charge of +5 (Hancock, 2000).

In 2013, the International Conference on Polymyxins established the "Prato Polymyxin Consensus"- the framework for optimizing the clinical use of

colistin and polymyxin B, which was refined in the following conferences (Lenhard, Bulman, Tsuji, & Kaye, 2019).

The population pharmacokinetics of colistin and polymyxin B were elucidated in 2011 and 2013 respectively, allowing the improvement of the dosage required for the intended plasma concentration. Colistin is administered in an inactive form (prodrug colistin methanesulfaonate, CMS) for it to be slowly converted into its active form, taking into account the patient's renal function for dosage determination, while polymyxin B (PMB) is not affected by renal function and is administrated in an active form, allowing its pharmacokinetics to be more predictable (Lenhard et al., 2019).

Of the two molecules, polymyxin B was chosen as the one to be studied in this work, as it is conventionally applied in an active form and, since it is shown to be less toxic, it has a broader therapeutic spectrum.

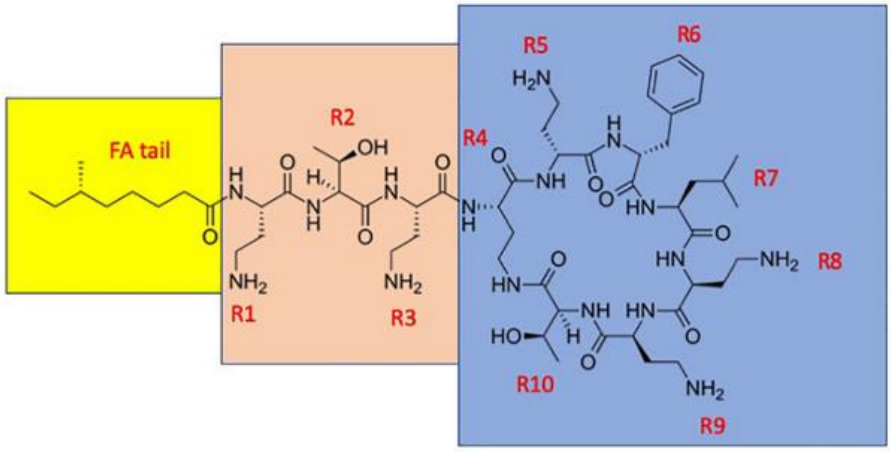

Figure 2- Chemical representation of a Polymyxin B molecule. The structure is composed of a cyclic portion (shaded in blue), a linear "panhandle" (in orange) and a fatty acyl tail (as yellow). In colistin, R6 D-phenylalanine is replaced by D-leucine. Adapted from Vaara, 2019.

The mechanism of action of these molecules (figure 2) starts with the binding to anionic groups like phosphate and pyrophosphate in lipopolysaccharides

(LPS) and lipids exclusive to outer membranes of Gram-negative bacteria, releasing them from the membrane by creating pores and compromising the integrity of the membrane. This allows periplasmatic components and external molecules to flow through (Vaara, 2019). This is followed by the damage of the cytoplasmatic membrane, leading to the leakage of components such as adenosine 5'-triphosphate (ATP) (Vaara, 2019). Possible additional effects include inhibiting the NADH-quinone oxidoreductase, thus producing hydroxyl radicals and reactive oxygen species (Vaara, 2019). Strains exposed to polymyxins, even if they are resistant against them, are sensitized towards other classes of antibiotics, allowing a synergistic combination of drugs (Lenhard et al., 2019; Vaara, 2019).

These molecules were considered too toxic for systemic use, due to nephrotoxic side effects (Hancock, 2000; Lenhard et al., 2019) thus making their research very limited since then (Lenhard et al., 2019). This toxicity is the result of reabsorption by the proximal tubular kidney cells, inside which the polymyxins inhibit the mitochondrial electron transport chain, that increase super oxide production and induce apoptosis by caspases activation (Lenhard et al., 2019; Vaara, 2019). There is an upregulation of cholesterol production that is thought to be an attempt to protect the cell. Several attempts to administrate antioxidants simultaneously to reduce nephrotoxicity have not produced data supporting the routine co-administration (Vaara, 2019).

Polymyxins re-entered clinical use as last-resort antibiotics, due to increasing instances of extremely multiresistant bacteria, specially *Enterobactericeae*, *Pseudomonas aeruginosa* and *Acinetobacter baumannii* (Lenhard et al., 2019; Vaara, 2019). Furthermore, their toxicity limits the dosage to suboptimal efficacy (Vaara, 2019). While most antibiotics from the "golden age of antibiotic discovery" have been replaced by new and improved versions, polymyxins remain part of the exceptions that do not have newer developed versions in clinical use (Vaara, 2019).

Their usage resurged against Enterobactericeae due to the spread of mobile plasmids encoding Carbapenemase (β-lactam degrading enzyme), that when acquired by strains with resistance mechanisms to other classes of antibiotics, leaving very few classes of drugs with active effects (Lenhard et al., 2019). This β-lactamase is not affected by conventional inhibitors, being addressed by next-generation β-lactamase inhibitors (Lenhard et al., 2019). Although they have been shown to improve the clinical outcome of patients, mortality remains high, so the clinical use may include polymyxins for the synergy, though preliminary studies have not shown results yet (Lenhard et al., 2019).

In combat of multidrug-resistant *Pseudomonas aeruginosa*, polymyxins are being replaced by safer anti-pseudomonal antibiotics. Nevertheless preliminary in vitro studies did show that there is synergy effects between some of them and polymyxins, but further research is needed (Lenhard et al., 2019).

Currently, the treatment of *Acinetobacter baumannii* is reliant on polymyxins unless drugs able to affect the β-lactam resistant strains, which by 2010, was the case in approximately half the clinical isolates of *A.baumannii* in the USA (Lenhard et al., 2019). Attempts are being made to improve treatment of A. baumannii infections, for example combination regimes of polymyxins with traditional antibiotics. Nonetheless there has not yet been a trial demonstrating effectiveness of such methods (Lenhard et al., 2019). The alternative is the development of novel antibacterials since the recently developed β-lactamase inhibitors are not effective against the enzyme oxacillinase that grants *A.baumannii* resistance, oxacillinase (Lenhard et al., 2019).

Polymyxin B nonapeptide is a derivative of polymyxin B that does not have the fatty acyl tail (Figure 2) and the N-terminal diaminobutyryl (DAB) (French et al., 2020; Lenhard et al., 2019). Instead of having bacterial activity, can make the outer membrane permeable to antibiotics that normally would not be able to enter the periplasm (Lenhard et al., 2019; Rose et al., 2000). In animal

testing, it showed less nephrotoxicity, but it is not going active clinical development (Lenhard et al., 2019).

SPR741 is a low toxicity analogue that also does not have bactericide activity, but instead is able to improve the effect of other antibiotics (French et al., 2020; Lenhard et al., 2019). It lacks a fatty acyl tail and has a lower positive charge (+3 compared to +5 of PMB) which change its activity but also improve its safety profile (French et al., 2020; Lenhard et al., 2019). It is being developed by Spero Therapeutic Inc, having completed clinical trials of Phase I (Lenhard et al., 2019).

MRX-8 is a polymyxin analogue whose fatty acyl is bonded with a ester bond, which can be hydrolyzed in the blood (Lenhard et al., 2019; Lepak, Wang, & Andes, 2020). It is the product of "soft drug design"(drug design which aims to develop safer drugs by designing the metabolism and detoxification of the compound), intended to create an analogue that is metabolized for less nephrotoxic metabolites after activity (Lepak et al., 2020), which has been shown to be less toxic to kidneys than polymyxin B in rats studies while maintaining the same effect (Lenhard et al., 2019). It is developed by MicuRx Pharmaceuticals, which has received 5.2 million dollars (Lenhard et al., 2019; Vaara, 2019).

Analogues have the potential to become therapeutic agents but few have reached clinical studies (Lenhard et al., 2019). The possibility of an analogue having less nephrotoxicity or more antibacterial potency would be an improvement for combating infections (Lenhard et al., 2019).

While safer alternatives to polymyxins are being developed, bacterial resistance to those drugs is also being developed (Lenhard et al., 2019). The polymyxin class of antibiotics may eventually be relegated to therapy in combination, whether as the current ones or as analogues, but presently they are still necessary as last line antibiotics (Lenhard et al., 2019).

Another antimicrobial peptide family, polyphemusins, which albeit not having the same medical history, have shown results in suppressing growth *in vitro* of both Gram-negative and Gram-positive bacteria, fungi and mammalian cancer cells (Marggraf et al., 2018).

The polyphemusin family are β-hairpin antimicrobial peptides that were discovered in hemocytes of *Limulus polyphemus*, the American horseshoe crab, that have a chain of 18 amino acids with 2 disulfide bonds and several lysine and arginine residues, which produce a high net positive charge, while being amphiphilic (Marggraf et al., 2018; Powers, Martin, Goosney, & Hancock, 2006).

Besides their broad spectrum of activity, they also have an affinity for LPS and may degrade biofilms of *Staphylococcus aureus* (Marggraf et al., 2018). Polyphemusin have preferential interaction with negatively charged membranes, being able to disrupt both outer and inner Gram-negative membranes and their cationic and amphilipathic properties are considered essential for their activity (Marggraf et al., 2018).

The polyphemusin family has 3 isoforms. Of them, polyphemusin III has the least bactericidal activity and the highest cytotoxicity (Marggraf et al., 2018). This toxicity is likely due to a higher hydrophobicity, which correlates to increase affinity towards all membranes (Marggraf et al., 2018). From the remaining, polyphemusin I was chosen for this work, as it is the most studied.

Polyphemusin I has a rapid killing effect (5 minute of contact) and a low minimum inhibitory concentration (sometimes lower than 1 μg per millilitre) and great affinity for lipopolysaccharides but affects greatly both Gram-negative and Gram-positive (Powers et al., 2006).

Although polyphemusin I is among the most effective antimicrobial peptides, there is not a consensus on the mechanism of action (Yurkova, Zenin,

Sadykhov, & Fedorov, 2020). Polyphemusin I induces flip-flop movements of membranes lipids, with a preference for negatively charged membranes (Powers et al., 2006). Studies have shown that Polyphemusin I bactericide effect comes in part from translocating the membrane and reaching the interior vesicles (Powers et al., 2006). Peptides from similar families, tachypesins, were shown to bind to DNA (Powers et al., 2006).

It has been established that it does enter the cell with minimal damage to the membrane and mainly targets intracellular components, rather than creating pores for molecule to enter or exit the cell (Powers et al., 2006; Yurkova et al., 2020). Tests of dimerization, which should decrease the number of molecules required to make a pore, did not change the Minimum Inhibitory Concentration (MIC), suggesting pore formation to not be the killing mechanism (Yurkova et al., 2020).

Polymers as delivery mechanism

Applications of AMPs *in vivo* faces a hurdle in achieving an effective concentration, as they can: i) be inactivated by binding to proteins, ii) cause toxicity or immune response by interacting with human cells, iii) be excreted by the liver and kidneys, and iv) undergo degradation in the highly proteolytic environment, such as infected tissues (Martin-Serrano et al., 2019; Nordström & Malmsten, 2017).

The goals of designing a delivery system is the reduction of toxicity, protection from biodegradation, and improving environmental stability and physiochemical properties (Dash & Konkimalla, 2012).

The conjugation of AMPs to polymers can preserve the function of both components, diminish undesired properties like cytotoxicity and/or improve the ones that lack stability (Martin-Serrano et al., 2019; Sun et al., 2018)

Polymers are molecules formed by the repetition of small units called monomers, whether natural like DNA or cellulose or synthetic like Polyethylene glycol (PEG) or PCL. In the last decades, the biomedicine and food industry have increasingly used biocompatible or biodegradable polymers (Martin-Serrano et al., 2019). Biodegradable polymers have the advantageous property that their metabolites can be eliminated from the body by innate metabolic processes (Dash & Konkimalla, 2012). There are several methods to apply polymers in biomedicine, such as polymer coated surfaces, nanofibers, and polymer conjugates (Martin-Serrano et al., 2019).

Functional polymers can be conjugated with AMPs to improve their properties (Sun et al., 2018). Conjugating AMPs with functional polymers enhances antibacterial activity, stability and selectivity (Sun et al., 2018). PEGylaction is able to increase circulation time by improving water solubility, reducing renal filtration and help AMPs avoid immune system cells (Sun et al., 2018).

Similar to traditional amphiphilic copolymers, AMP-polymer conjugates can be designed to self-assemble into various nanostructures such as nanosheets, micelles, nanoparticles or vesicles (Sun et al., 2018). There are many potential applications of nanostructures of AMP-polymer conjugates, such as antibiofilm, implant coating, wound dressing, drug delivery and more (Sun et al., 2018). Nanostructures have shown advantages in many fields, and AMPs can further improve these advantages (Sun et al., 2018). AMPs conjugates in nanoparticles demonstrated to have a better performance than their conventional counterparts (Sun et al., 2018).

The therapeutic treatment of infection would benefit from the synergy between AMPs-polymer conjugates and traditional antibiotics, as it may be an effective way to prevent resistance from developing, and result in better antimicrobial effects than individual components (Sun et al., 2018).

The properties of both the polymer and the bond to the AMP can influence the antibacterial activity of the conjugate, and can be engineered to respond to pH or temperature (Sun et al., 2018) .

The plurality of production methods allow a big arsenal of polymer variants with different properties in assembly behaviour, drug loading, and cellular uptake, which allows fine-tuning according to the therapeutic need (Grossen, Witzigmann, Sieber, & Huwyler, 2017). Nanoparticles can be modified to specifically interact with a target by including a ligand that has selective interactions such as antibodies (Grossen et al., 2017). However over-engineering structures can be detrimental as excessive chemical modification may decrease biocompatibility or effectiveness (Sun et al., 2018).

Amphiphilic AMP-polymer conjugates can organize themselves into micelles where the AMP is either the core or corona (Sun et al., 2018). Polymeric micelles are nano-sized particles that are formed by amphiphilic polymer self-assembling into a usually spherical structure in monophasic or biphasic liquid (Dash & Konkimalla, 2012). There have been extensive studies of micelle properties such as shape (Debye, Anacker, & Anacker', 1950; Tanford, 1972) and formation (Phillips, 1954; Tanford, 1974).

Micelles that use AMPs as building blocks have potential as therapeutic agents because they are "armed", which can be combined with drugs loaded in the micelle for multiple effects (Sun et al., 2018).

An example of environmental response is a micelle with an AMP block that is only positively charged in a lower pH than the blood, such as a tumour site (Sun et al., 2018).

It is possible to improve upon conventional drug formulations using polymers, in multiple form such as crosslinked polymers, polymeric micelles or multiple component polyplexes (Liechty, Kryscio, Slaughter, & Peppas, 2010). Modern

research is supplementing traditional drug development with methods to improve both new and existing. One of these methods is the application of polymers as delivery systems, which can be designed to improve drug formulations in various ways, such as increasing effectiveness and targeting specific tissues (Dash & Konkimalla, 2012).

Micelles are the product of the amphiphilic behaviour of compounds in water, as they self-assemble into a structure, usually spherical, where the hydrophobic components form the core and the hydrophilic surface (Kedar, Phutane, Shidhaye, & Kadam, 2010). These structures can be used to transport substances and designed to target specific cells or having a controlled substance release (Kedar et al., 2010; Seidi, Jenjob, & Crespy, 2018).

Micellar delivery can be achieved with either the inclusion (loading) of apolar/hydrophobic drugs in the micelle core (Shuai, Ai, Nasongkla, Kim, & Gao, 2004), or bonding the drug is to the micelle components, with both methods being able to improve drug solubility (Owen, Chan, & Shoichet, 2012). Further modifications can improve the formulation of the micelle molecules, such as adding compounds to the core such as benzyl groups to increase hydrophobicity, or crosslinking to decrease the number of molecules needed to create a stable micelle (Lu, Zhang, Yang, & Cao, 2018)

In this work the micelles were made with the AMP as hydrophilic components, as they are charged and water-soluble, and as PCL is not charged, it will not interfere with the bonding process, so that the conjugate AMP-PCL will be able to exhibit its membrane disrupting mechanism.

In this work the polymer that will be used is PCL, because it is biocompatible and bioresorbable, i.e., can be metabolized and eliminated by the biological processes of an organism (Lam, Hutmacher, Schantz, Woodruff, & Teoh, 2009), and has been used in many different biomedical applications with

success. For example, as a scaffold for tissue repair (Martinez-Diaz et al., 2010) and transporting of medication in the form of micelles (Shuai et al., 2004).

Polycaprolactone is a semi-crystalline, biodegradable aliphatic polyester, where the principal monomer used is ε-caprolactone (ε-Cl), a synthetic commercially available compound (Grossen et al., 2017; Mandal & Shunmugam, 2020). Other isomers are found in nature such as γ-Cl (moiety of floral scent molecules) and δ-Cl (found in heated milk fat) (Mandal & Shunmugam, 2020). PCL is explored in studies of diverse applications, such as medical devices and tissue engineering, thanks to its biodegradability, biocompatibility and cost-effectiveness (Grossen et al., 2017; Mandal & Shunmugam, 2020).

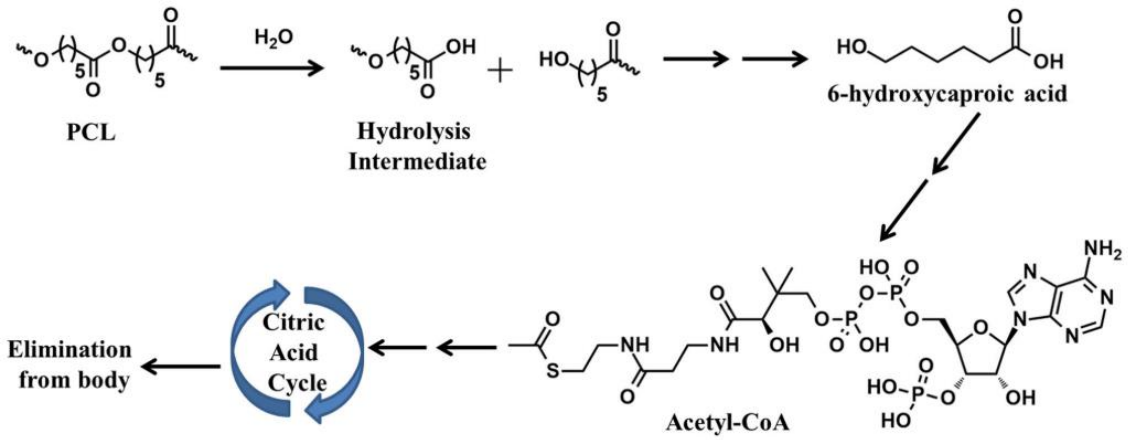

Figure 3- Schematic representation of the metabolization of PCL (Mandal & Shunmugam, 2020)

The degradation of the ester links is self catalyzed by free carboxylic groups, occurring at physiological conditions, and producing 6-hydroxycaproic acid which is converted to acetyl-CoA and enters the citric acid cycle (Grossen et al., 2017; Mandal & Shunmugam, 2020). In biotic environments, enzymes, mainly esterases and some lipases, have a role in catalyzing this reaction (Mandal & Shunmugam, 2020).

PEG-PCL micelles remain stable for months in phosphate buffered serum, but in the biological medium they are affected by protein opsonisation (Grossen et al., 2017). In animal studies, PEG-PCL unimers were removed from plasma with a half-life of 10.2h, where micelles lasted triple of the time, and no accumulation of metabolites was observed as they were excreted from the body (Grossen et al., 2017).

Enzymes as biocatalysts

Enzymes are biological catalysts that are advantageous over conventional metallic catalysts because of their exceptional product selectivity, mitigation of waste generation, ability to function at mild conditions, lower energy requirements, simplified production routes and lower toxicity (Chapman, Ismail, & Dinu, 2018).

Enzymes are applied in many industries such as food and beverage, detergent, pharmaceutical, and bio fuel (Chapman et al., 2018). Their application is projected to grow with the improvement of the economics of their use, with the global enzyme market projected to reach 6.32 billion dollars in 2021 (Chapman et al., 2018). Most enzymes in use are hydrolytic, mainly proteases followed by carbohydrases (Kirk, Borchert, & Fuglsang, 2002).

Modern biotechnology is the origin of the contemporaneous application of enzymes, where natural enzymes from spontaneously growing microorganism were applied in the production of food like cheese, bread, beer, wine, vinegar, and commodities like leather, indigo and linen (Kirk et al., 2002).

During the last century, the production of enzymes as select strains, purified and well-characterized, even in large amounts, allowed them to become viable products and catalysts in the industrial context, for example in detergent, textile and starch industries (Kirk et al., 2002).

The production of recombinant gene cells, allowed for further improvements

in the production of established enzymes and the manufacture of new enzymes from microorganism that cannot be cultivated yet (Kirk et al., 2002).

Protein engineering allowed enzymes to be tailor made for new reactions and specific conditions (Kirk et al., 2002). The improvements in protein design directed evolutionary approaches also allowed the production of better enzymes with improved activity, stability, and substrate affinity and cheaper isolation (Chapman et al., 2018). Directed evolution utilizes random modifications to the amino acid sequence, then the mutants are screened for improvements, and the beneficial alteration is further improved on, which has produced variants able to function in extreme pH or high temperatures and some have reached several orders of higher catalytic activity (Chapman et al., 2018).

Molecular dynamics (MD) simulations can provide understanding of the phenomenon that determines the enzymes physical and catalytic characteristics, at an atomic level (Chapman et al., 2018). These simulations apply Newton's laws of motion at the atomic scale, providing insight into interactions such as the binding mechanism, which led to the optimization of the studied enzymes (Chapman et al., 2018).

The main application of enzymes is the detergent industry, which is constantly improving the current engineered version of the detergent enzymes to fit ever-updating performance requirements (Kirk et al., 2002). This includes the ability to fulfil their role at lower temperatures and alkaline pH (Kirk et al., 2002). The development of detergents that are both cost-effective and environmentally benign relies on enzymes, not as a catalyst for a step in production but as a product (Chapman et al., 2018). The specificity of enzymes also avoids the damage to fabrics and surfaces that harsh detergent agents can cause, and the ratio of enzymes in a detergent mixture can be fine-tuned for a specific application (Chapman et al., 2018)

In the pharmaceutical industry product specificity is a high priority, so enzymes' high selectivity allows production with less effort to purify the desired stereoisomer and lessen the use of high temperatures or chemically harsh substances (Chapman et al., 2018).

Traditional chemical synthesis, with metallic catalysts, is not viable in food production due to toxicity, but enzymes are an alternative that allows for simple, safer, and efficient production (Chapman et al., 2018).

In the production of animal feed, there are enzymes turn components otherwise indigestible for monogastric, such as cellulose into digestible sugars, decreasing the amount of feed needed, or increase the uptake of phosphorus to prevent environmental release (Kirk et al., 2002).

The industries where excess waste is punished monetarily by aregulatory agency, such as paper, textiles, leather and biofuel, are expected to embrace more the use of enzymes along with progress (Chapman et al., 2018). For example, in textile industry, enzymes allow for cotton scouring to be performed at lower temperatures with less water consumption (Kirk et al., 2002). From an ecological perspective, enzymes like lipases, esterases, and proteases, which have the ability to hydrolyse ester bonds, are interesting means of bioremediation in cases of industrial waste contamination (Melani, Tambourgi, & Silveira, 2020).

However the application of enzymes is limited by their lack of stability at high temperatures, turbulent reaction systems and some industrial solvents (Chapman et al., 2018).

Enzymes can be improved for a task by immobilization, the attachment to the desired material, which can improve activity and stability in conditions outside the range of the free enzyme and imparts new functionality according to both the method of immobilization and the physical, chemical, electrical or

mechanical properties of the material (Chapman et al., 2018). Immobilized enzymes also reduce the number of steps required for processing as it is simpler to remove the catalyst from the reaction mixture, they maintain their catalytic ability and can be reused, even if the immobilization is time-consuming and costly (Chapman et al., 2018).

The industrial application of enzymes is associated with decreased consumption of energy, reduced chemical input and lower waste production, indicating the potential for enzymes to make industry both more eco-friendly and lucrative (Chapman et al., 2018).

For the reactions in this work, the enzyme class chosen was lipases, more specifically *Candida antartica* lipase B (CalB).

Lipases are serine hydrolases whose catalytic activity includes the hydrolysis of triaglycerols, synthesis of esters and transesterification and aminolysis (Navvabi, Razzaghi, Fernandes, Karami, & Homaei, 2018), but can be used to catalyse reactions of esterification, transesterification, interesterification, amidation, transamidation, aminolysis, aldol condensation, and Michael addition (Jiang & Loos, 2016). Lipases are most active on long-chain fatty acids, namely ten or more carbon atoms (Navvabi et al., 2018).

The active site is composed of the classic catalytic triad composed by a serine, histidine and aspartate residues (Melani et al., 2020). The aspartate residue is sometimes substituted by a glutamic acid, another catalytic acidic residue (Jiang & Loos, 2016). Lipases are stable even in non-aqueous solution, and do not require a cofactor (Melani et al., 2020). They have high activity and most have a alkaline optimum pH, at 8 to 9 (Melani et al., 2020).

Lipases have a characteristic α/β hydrolase fold that grants the distinguishing property of interfacial activation, as the enzyme conformation is obtained in contact with an oil-water interface so the lipase operates in the interface of

biphasic systems (Goswami & Van Lanen, 2015; Melani et al., 2020). In aqueous media the hydrophobic active site is blocked by a lid with an internal hydrophobic face and external hydrophilic face (Melani et al., 2020). However not all lipases have this lid, so they do not have interfacial activation (Melani et al., 2020).

Commercial lipases were obtained from the fungi genera *Rhizopus*, *Candida* and *Rhizomucor* and the bacteria genera *Pseudomonas* and *Choromobacterium* (Navvabi et al., 2018), with the most used being CalB, thanks to its versatility (Goswami & Van Lanen, 2015).

Computational Methods

Molecular Mechanics

Molecular Mechanics (MM) calculations provides a way to simulate large and complex molecular systems without the massive resource consumption of Quantum Mechanics calculations that overwhelm even supercomputers (Durrant & Mccammon, 2011). The calculation of the forces in the system is achieved with a simplified potential function (equation 1, Case et al., 2020) using bonded and non-bonded terms. When solving the potential function, the variables are replaced with parameters obtained with theoretical calculations or determined experimentally according to atom types, element and chemical environment (Y. Wang, Fass, & Chodera, 2020).

$$E_{total} = \sum_{bonds} K_b(r - r_{eq})^2 + \sum_{angles} K_\theta(\theta - \theta_{eq})^2 + \sum_{dihedrals} V_\phi[1 + \cos(n\phi - \gamma)] + \sum_{i=1}^{N-1} \sum_{j=i+1}^{N} \left[\frac{A_{ij}}{R_{ij}^{12}} - \frac{B_{ij}}{R_{ij}^{6}} + \frac{q_i q_j}{\varepsilon R_{ij}}\right] \quad (1)$$

In this work, the force fields used are AMBER's ff14SB, AMBER lipid17 (Dickson et al., 2014) and the General Amber Force Field (GAFF) (Sprenger, Jaeger, & Pfaendtner, 2015; J. Wang, Wolf, Caldwell, Kollman, & Case, 2004) which were obtained for proteins and lipids respectively, with the later offering support to non-included residues -by using AMBER antechamber tools to

adjust atom types and add missing parameters (Javanainen & Martinez-seara, 2016; Maier et al., 2015; Salomon-ferrer, Case, & Walker, 2012). For the membrane simulation, the CHARMM force field was used, as it was the one employed by the software that constructed the membrane. CHARMM force fields are similar to amber force fields but they are not compatible because non-bonded parameter development follows different strategies (Vanommeslaeghe et al., 2009).

The terms labelled bonds, angles, and dihedral are the bonded terms, which are related to the covalent bonds between atoms. The first is the distance between atoms, the second is the angle between atoms and the third is the dihedrals (ϕ) the angle between the planes defined by two sets of three atoms, as illustrated in figure 4. These variables in the simulation are compared with "eq" are the ideal values for the atoms, i.e., most stable configuration; and a constant K for stiffness (the larger, the more energy is required to move away from the ideal) (Harrison et al., 2018; Langham & Kaznessis, 2010). These variables are defined as the balance of attracting and repelling forces between atoms, and the more stable (least energetic the point of equilibrium), the more energy is required to move away from that point.

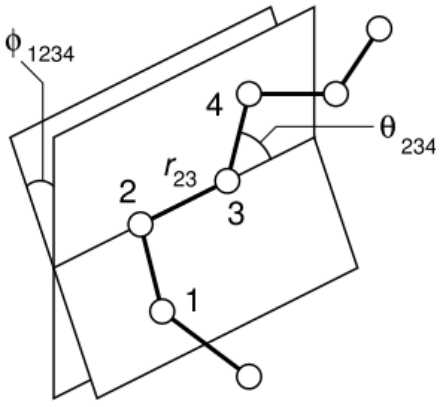

Figure 4 - Visual representation of bond (r), angle (θ), and dihedral (ϕ) with atoms 1 to 4, the number of each represent the atoms involved. Adapted from Sharma, Kumar, & Chandra, 2019.

Non-bonded terms account for van der Waals and electrostatic interactions, which are calculated using the Lennard-Jones potential and Coulomb's law respectively (Durrant & Mccammon, 2011). They cover the distant interactions by atoms either not connected or that are at a distance greater than three covalent bonds. Although for atoms distant enough that the vdW interaction can be ignored, there is a cut-off to reduce the number of calculations (Langham & Kaznessis, 2010). This is not precise in electrostatic interactions, so after the cut-off, the Ewald summation is applied and, distant interactions are modelled with Fourier transform to reduce workload (Stenberg & Stenqvist, 2020).

Quantum Mechanics

Any simulation that requires a change in the quantum electronic structure of the material, to break or create chemical bonds, requires Quantum Mechanics (QM) calculations (Mendieta-moreno & Marcos-alcalde, 2015). QM, as a methodology, describes the behaviour of individual particles, including electrons, with time dependent Schrödinger's equation (equation 2, Levine, 2000) as a means of calculating the position of the electron in a wave function as a probability (Engel & Dreizler, n.d.).

$$-\frac{\hbar}{i}\frac{\partial\Psi(x,t)}{\partial t} = -\frac{\hbar^2}{2m}\frac{\partial^2\Psi(x,t)}{\partial x^2} + \mathrm{V}(x,t)\Psi(x,t) \tag{2}$$

In equation 2, ħ (called "h bar") is the Plank constant (h) divided by 2π (two times pi), Ψ is the wave function with coordinates of particle x at time t and i stands for $\sqrt{-1}$.

This equation cannot be directly used in calculations for a system as it is for a single particle, but some formulations can be applied to a complete system, such as Born– Oppenheimer approximation, where the motion of

electrons and nuclei is partially depopulated due to the difference in timescale (Engel & Dreizler, n.d.; Levine, 2000).

While all quantum calculations are more computationally demanding than any force field to the point of impracticality on any large system (Y. Wang et al., 2020), *ab initio* methods are so resource demanding that they are reserved to the most complex or accuracy-demanding cases, and Density Functional Theory (DFT) is used in most works (Thiel, 2009; Mardirossian & Head-gordon, 2017).

With DFT, electronic energy is calculated with a functional of the density of electrons instead of a many-body electronic wavefunction (Neese, 2009). The basis of modern DFT are two theorems by Hohenberg and Kohn: 1)all ground-state properties of an electronic system is determined by the ground-state electron density uniquely and 2) a functional of the electron density is a minimum for the ground-state density can describe the energy of an electron distribution (Neese, 2009).Rather than calculate a many body equation, in DFT, the calculations rely on minimizing the density functional (Neese, 2009).

Quantum Mechanics/Molecular Mechanics

The hybrid Quantum Mechanics/Molecular Mechanics (QM/MM) is a method that allows a less resource intensive simulation while maintaining accuracy, by limiting QM to a section of the system where the reaction happens, while MM is applied to the remaining system (Gerrit Groenhof, 2013).

QM/MM coupling the methods can be subtractive, where the interaction is modulated entirely in molecular mechanics, as MM is applied to the whole system and also to just the subsection for the quantum calculations and is then subtracted to avoid double counting of the area (Groenhof,

2013; Thiel, 2009); or additive, where molecular mechanics is not applied inside the quantum section but requires correction for the interactions and bonds that cross the borders between sections (Groenhof, 2013; Thiel, 2009). While subtractive coupling is simpler to implement, the QM section may not have a compatible force field, or it cannot support chemical changes from the reaction (Groenhof, 2013; Thiel, 2009). On the other hand, additive methods requires explicit terms for the interactions between subsystems : mechanic embedding in which the force field is adjusted to not allow the QM section to be polarized by the environment of the MM section, which is not the best method for biomolecules, as they can be highly polar (Groenhof, 2013; Thiel, 2009); or electrostatic embedding in which the electrostatic interaction between subsystems is calculated alongside the electronic wave function treating charged atoms of the MM section as one electron term, allowing the QM subsystem to react to the environment and mimic reality better (Groenhof, 2013; Thiel, 2009).

Molecular Dynamics

Molecular Dynamics (MD) simulations calculate the movement of atoms according to classical laws of motion. By calculating the sum of forces applied on an atom, it is possible to determine acceleration and by applying the laws of motion, it determines the position as a function of time (Langham & Kaznessis, 2010). Each atom is moved to the new position, updating the model to have a position corresponding to after a small interval of time in the order of femtoseconds (fs) (Durrant & Mccammon, 2011).

MD simulation's starting models can be provided by many different techniques, such as X-ray crystallography or nuclear magnetic resonance (Hollingsworth & Dror, 2018), or be custom built in software.

The molecular dynamics first step is the preparation of the system that is going to be simulated. In this work, that was accomplished with LEaP (link, edit and parm), a tool built in AMBER software package, which can set the force fields that are used, bond atoms (for example sulphite bridges have to be bonded manually) and solvates and adds ions to the system.

The simulations' environment in this work were run with water as the solvent, because it is the environment in which the conjugate will be applied and the standard solvent for enzymatic reaction. It was also applied periodic box conditions, in which the system is simulated as infinite copies of the primary simulation box, side by side. Only the atoms of primary box are tracked but interactions are simulated across boxes to include atoms within cut-off distance. The atoms leaving the primary box are replaced by the equivalent atoms entering from the opposite side, keeping the pressure constant while better mimicking real-world conditions. The starting kinetic energy of each atom was randomly assigned from a Boltzmann distribution.

Python programming language

Python (Python Software Foundation, www.python.org) is a free, open-source, cross-compatible and beginner-friendly programming language (Millman & Aivazis, 2011). Python is an interpreted language, rather than a compiled one, so it runs on a virtual machine to be independent of operating systems; it is dynamically typed, where using variables does not require declaring their type for the compiler, making it easier for beginners. Python error messages can be easily searched in the internet to understand what went wrong.

Instead of using parenthesis { } to delimit sections of code, python uses indentations, which are more readable for beginners. By using indentations with conditionals (the "while" and "for" conditions), it is possible to set a loop

to run a block of code multiple times until the condition is reached. Using if/else conditions, it is possible to run a block of code when appropriate.

The many available modules allow the user to extend the capabilities of python without needing to code them. Of the available modules the ones used were: Numpy to extend the numerical operations (Harris et al., 2020), Pandas to process and analyse data (McKinney, 2010), Matplotlib, a library of utilities for visualization, more specifically Pyplot, a sub-module for graphical representation(Hunter, 2007).

Using Pandas it is possible to load data into columns to be edited and processed. In this manner it is possible to maintain the connection between values while applying functions such as sorting or mathematical operations.

The Numpy module was used in this work mostly for the trigonometry functions is provides. Said functions were used to make the spherical custom micelle model.

The Pyplot sub-module allowed the better awareness of the coordinate processing, by enabling the visualization using a three dimensional graph.

Micelle trajectory analysis

The polymer of this work was chosen, among other characteristics for its ability to self-assemble into micelles when in water (Raman, Pajak, & Chiew, 2018). There is still necessary to characterise the properties of this specific micelle. Several mathematical means of evaluating the structure of micelles such as eccentricity, the radius of gyration, solvent accessible surface area (SASA), and internal hydration (Faramarzi et al., 2017; Lebecque, Crowet, Nasir, Deleu, & Lins, 2016).

The shape of a micelle is evaluated by how much it deviates from an ideal spherical form. Eccentricity (e) is a unitless measurement of that

deviation, the lower it is the closer to the ideal shape, and is calculated with equation 3 , where l_{min} and l_{avg} are respectively the minimum (min) and average (avg) moments of inertia along the principal axis (Krüger & Kamerlin, 2017; Lebecque et al., 2016), determined by diagonalization of the inertial matrix from the specified atoms coordinates with CPPTRAJ tool command "principal".

$$e = 1 - \frac{l_{min}}{l_{avg}} \quad (3)$$

The radius of gyration is a measurement of the distribution of atoms relative to the center of mass. The effective radius of a micelle can be obtained by multiplying the radius of gyration by $\sqrt{\frac{5}{3}}$ (Krüger & Kamerlin, 2017). Experimental measurements of the radius of gyration tend to yield larger measurements when compared to simulations due to including water molecules in the hydration shell (Faramarzi et al., 2017). It is calculated with the CPPTRAJ command "radgyr".

The solvent accessible surface area represents the area of vdW that is exposed to the environment and therefore, able to be interacted with. There are two ways of calculating SASA: the Connolly method calculates the surface area by simulating a probe moving across the surface to determine what is the shape of the molecule surface (Connolly, 1983); and the LCPO (linear combination of pairwise overlaps) method that calculates an atoms overlap of vdW radii to subtract from the total, with correction terms to avoid errors from multiple overlaps (Weiser, Shenkin, & Still, 1998). These methods are calculated with the CPPTRAJ tool, the commands "molsurf" and "surf" respectively.

Internal hydration or hydrophobic tails hydration is a debated subject as molecular simulations do not show noticeable amounts of water in the

micelle core but experimentally it appears to be noticeably hydrated (Faramarzi et al., 2017). It is calculated as the average number of water molecules in proximity to hydrophobic components of the micelle with the CPPTRAJ tool command "watershell".

Results and discussion

Molecular modelling

The AMPs molecular models were obtained from the RCSB Protein Data Bank archive, a database that contains information, including structure models, for biological macromolecules (Burley et al., 2019; Goodsell et al., 2020). The structural files were prepared for simulation by the AMBER tool LEaP, which is the principal tool to create and edit systems for simulation. LEaP allows choosing what force fields to use, adds missing atoms according to reference files, and enables editing structures such as adding bonds.

The pdb code for the structure of Polyphemusin is 1RKK, obtained with NMR and deposited by Powers, Rozek, & Hancock, 2004. The file was edited for the cysteine's disulfide bridges to be CYX (bonded) rather than CYS (free form), and manually bonded the residues 4 to 17 and 8 to 13, and the C-terminal amination was renamed to match the AMBER force field terminology.

Polymyxin B was not available by itself, but included in complex with a different protein, LSD1-CoREST1, in pdb code 5L3F (resolution 3.50 Å) obtained with X-ray diffraction and deposited by Speranzini et al., 2016. Since it is not a standard protein but rather a non-ribosomal peptide with modified amino acids, the AMBER tool antechamber was used to generate topology information which was saved as a file in the mol2 format that includes bond and charge information.

The structure for polycaprolactone was previously custom made in molecular design software for another project (Almeida, Figueiredo, & Carvalho, 2019)and was used in strands of 5 monomers.

Building base conjugate & Micelle first attempt

The conjugates were made by connecting the N-terminal amino acid of polyphemusin I to polycaprolactone's distal carboxyl group as shown in figure 5 (A). In studies with AMP-chitosan conjugates, the orientation of the peptide relative to the backbone influences the activity of the conjugates, with N-terminal linkage showing more antibacterial activity (Sun et al., 2018).

Due to polymyxins lack of n-terminal, the bond was made using a side chain nitrogen atom of polymyxin B that doesn't interact with the membrane (Velkov, Thompson, Nation, & Li, 2010) to the same atom of PCL, as shown in figure 5 (B).

(A)

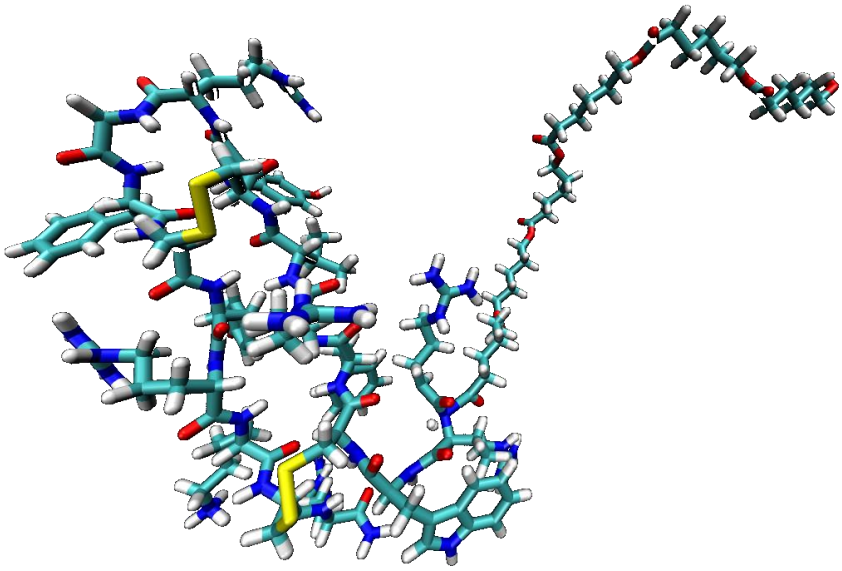

(B)

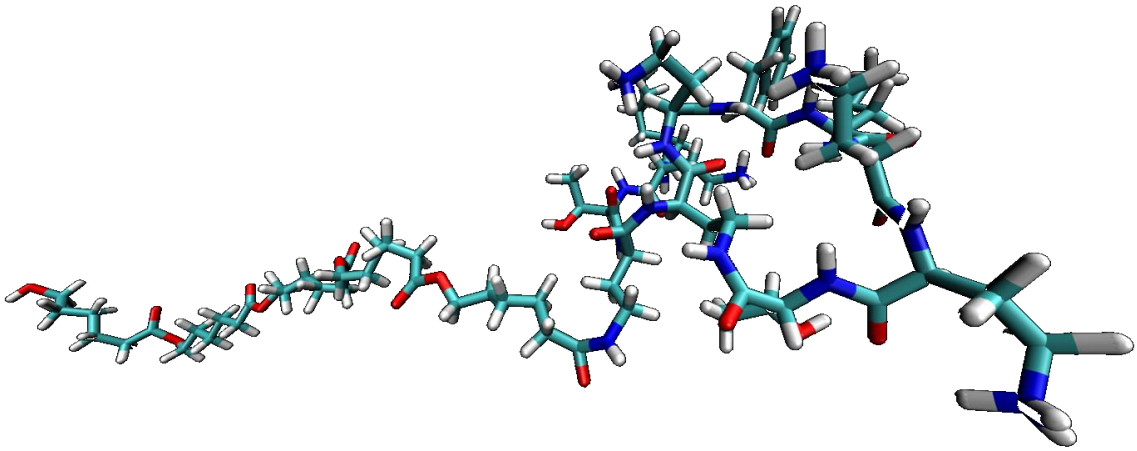

Figure 5- Images of the conjugated starting structures before molecular dynamics, polyphemusin I (A) and polymyxin B (B).

They were simulated in water to closer match the environment in which they are intended to be applied. To spare computational resources we started the simulation near the theoretical micellar optimum position, the choice of start the simulation near the optimum position, hoping to reduce the required time to reach equilibrium.

The conjugates were distributed in a starting position that approximates the final micelle structure by using CHARM-GUI input generator micelle builder (Cheng, Jo, Lee, Klauda, & Im, 2013; Jo, Kim, Iyer, & Im, 2008), which produced a structure file whose atoms positions were used as a basis. The molecule for the base structure, an Alkyl-PEG referred to as C13EG8, was chosen because it had enough atoms for the entire PCL chain without branching or ring atoms and still had room for three atoms of the AMP, so LEaP could use as basis to add the remaining atoms.

The micelle was composed of thirty molecules, and required the order of some atoms in the file to be switched as the input generator ordered atoms starting in the middle of the molecule and counting towards the extremities, first the alkyl part then the PEG. This led to a residue per molecule being split into two

parts that appeared separated in the file. As a consequence LEaP interpreted it as being two different residues and misplaced atoms in excess.

The molecule was edited manually using Microsoft® Excel to alter the main chain atom types and residue names to the intended names, repositioning lines, and using the option to save as space separated values to maintain the columns in the pdb format. However manual editing was very error-prone and many corrections were required to create the final working file.

The first AMP to be tested was polymyxin B because it is the most medically relevant of the two AMPs.

LEaP produced a micelle system that would crash during the heating step, and multiple variations, including systems with fewer conjugates, were used for troubleshooting. The issue was the double bond oxygen atoms of the carboxyl group placed by leap being too close to the main chain oxygen, which yielded a very high energy that couldn't be computed. The solution was to perform more minimization steps using a mask (atom selection) where only the oxygen atoms are allowed to move.

However, the micelle was not stable and the molecules drift apart, as seen in figure 6, most likely due to the high positive charge of Polymyxin B. The solution was to have PCL molecules without AMP acting as stabilizer to the micelle by increasing the interaction inside the micelle core. The ratio chosen to attempt this was 1:1, making the micelle composition thirty chains with AMPs and thirty chains without.

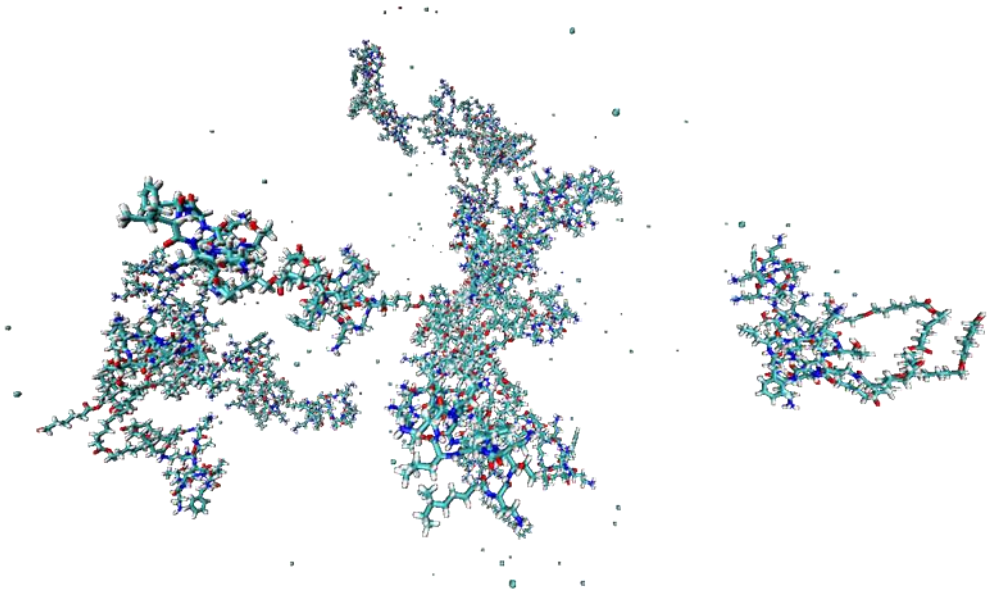

Figure 6- Image of the conjugated molecules after 20 nanoseconds of simulation. The molecules have been separated by the repulsion of the positive charges.

The chains without AMP in further works may be modified to improve the micelle stability of effectiveness, but for this work, the structure is a proof of concept, so simplicity is the most productive option.

Python Attempt File Editing

The 60 molecule micelle structure file was too big to be edited manually so the best way to proceed was to use the programming language python to automate the process.

Using the Pandas module (McKinney, 2010), the file information, skipping the header, was loaded into the columns of a dataframe:

- 'recordtype' for the information for the type of record of the line ("ATOM" for atoms, "TER" for the end of a molecule);
- 'number' for the atom number in the sequence;
- 'name' for the atom's chemical designation;
- 'resname', for the designation of the atom's residue;
- 'resid' for the residue's number;
- 'x', 'y' and 'z' for the coordinates of the atom.

The coordinates of x, y, and z were used to create a column (referred to by the designation of 'distance') of values calculated as the addiction of the coordinates squared, which is an adaptation of the equation to determine the distance between points in Cartesian coordinates (equation 4), when one of the points is the origin (0, 0, 0). The square root was omitted because the values maintain the same sequence. Therefore the calculation is simplified to shorten calculations.

$$d = \sqrt{(x_1 - x_2)^2 + (y_1 - y_2)^2 + (z_1 - z_2)^2} \quad (4)$$

The lines in the dataframe were ordered with the sort_values() function by resid to prevent mixing molecules and distance to place the atoms in order of proximity by how close they are to the origin. Then the number of the atoms and their name were corrected to match the intended molecule.

This did not work because of curves in the molecule that made atoms to be placed closer than the preceding atoms when they should have been further away, leading to a zigzag placement of atom, shown in figure 7 that resulted in errors when attempting to calculate the energy of those bonds.

(A)

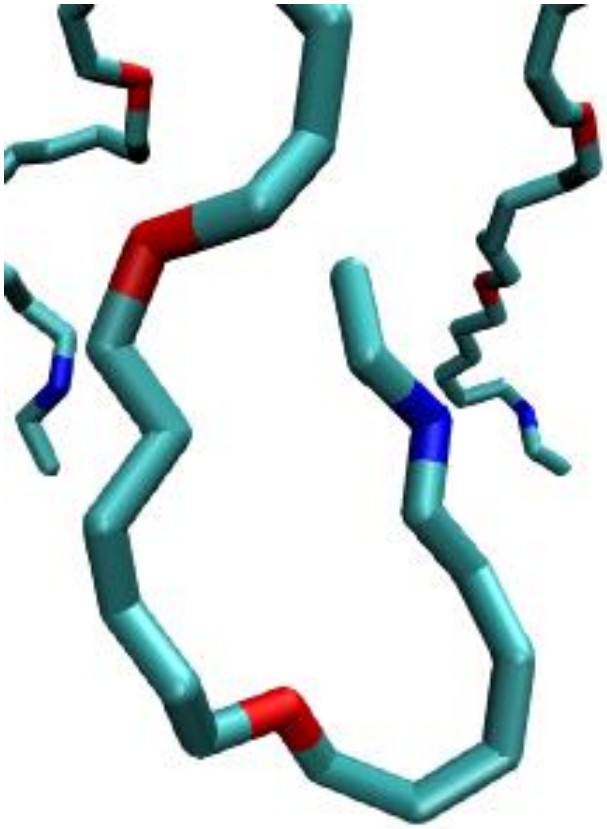

(B)

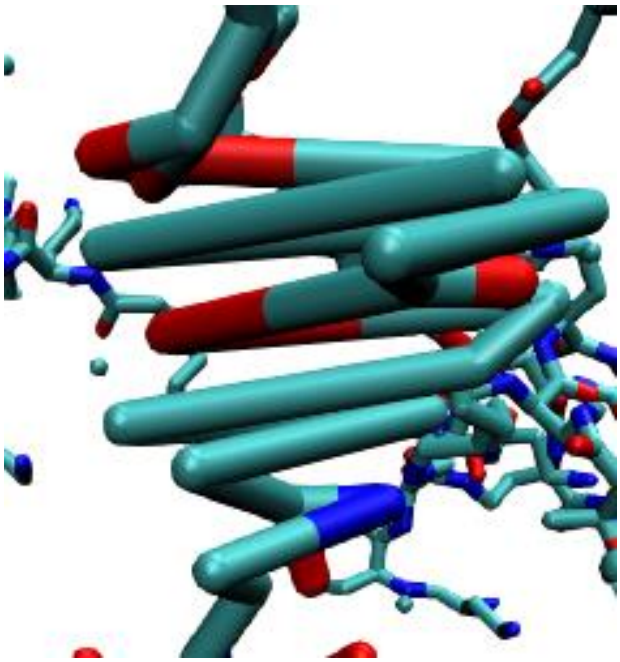

Figure 7- The end point of a PCL chain with the AMP at the extremity, before (A) and after (B) using the sorting python code and LeAP.

Python attempt Micelle builder

An alternative to the previous procedure was to use a custom micelle builder that could place the already edited molecules in a spherical arrangement. To achieve this goal, the coordinates were transformed into spherical coordinates, because they can be rotated around the origin whilst maintaining relative positions of atoms.

To make the micelle two functions to convert the coordinates to Spherical and to turn them back to Cartesian were made based on online sources, shown in ANEX II- Part 1. Spherical coordinates use a value for distance to origin (radius) and two angles, azimuth (angle with the x-axis in the xy plane) and inclination (angle of radius with the xy plane).

The original molecule distribution was based on the combination of possible azimuths and inclination angles with more than 60 results by using the angles $\pi/6$, $\pi/3$, $\pi/2$, $2\pi/3$, $5\pi/6$, $7\pi/6$, $4\pi/3$, $3\pi/2$, $5\pi/3$, $11\pi/6$, 2π. The function itertools.combinations_with_replacement() was used to make a list of points to place the molecule. However the placement was flawed and resulted in the superposition of molecules. An alternative method, shown in ANEX II-Part 2, was used that places the points evenly and can be scaled up to more easily. The method is based on an algorithm that places the atoms by in small increments to achieve a spherical shape while keeping the points apart. This metod allows for an even spacing of the points across the sphere, were the original placed them closer near the top and bottom, as seen in figure 8.

(A)	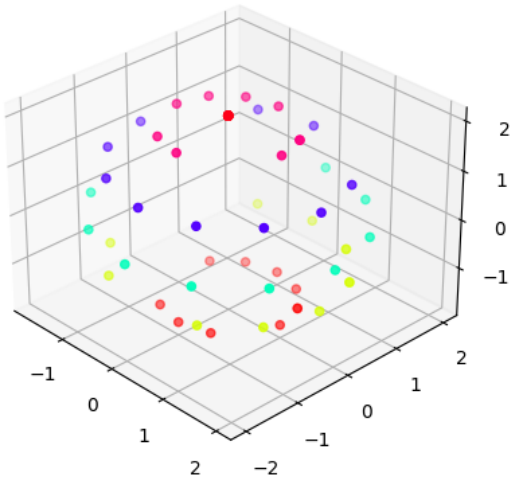
(B)	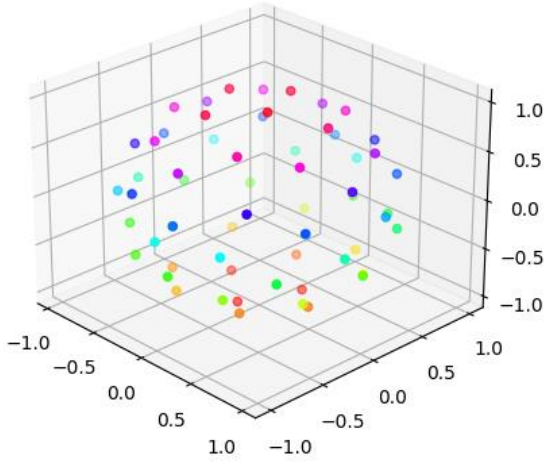

Figure 8- Comparison of both methods of point generation displayed using the module matplotlib.pyplot. (A) is the first method (combinations) and (B) is the alternative method.

The molecule used to rotate was aligned to the x-axis for simplicity, then the coordinates converted to Spherical and for each molecule until the desired amount, the Azimuth and Inclination of a point are added to the atom's coordinates. The output is rewritten with the string formatting option to space and align the columns to make sure the decimal cases are according to pdb format.

This method did not scale well to the amount of molecules required. The micelles produced have overlaps, which yield incalculable energy in repulsive

forces. An attempt to produce linear molecules to be adjusted by minimization also did not work because the bonds were too stretched and the energy calculation became equally incalculable. So for the sake of time the 60 molecule micelle was redefined to use the functional but unstable micelle file and reduce the number of antimicrobial peptides to obtain the same AMP.

So the micelle with thirty AMP was edited to have only fifteen AMP. A short python code was written to copy the pdb file line by line and count the number of atoms with the residue name of the AMP, until the desired amount was reached to then skip the remaining AMP atoms. The micelle was simulated for 20 nanoseconds in segments of two and a half nanoseconds, during which it remained stable. This method was repeated to create a micelle without AMP as a control and simulated during the same amount of time (20 ns) in the same conditions to be used in structural comparisons. Both can be seen in figure 9, with the starting position for comparisson

(A)

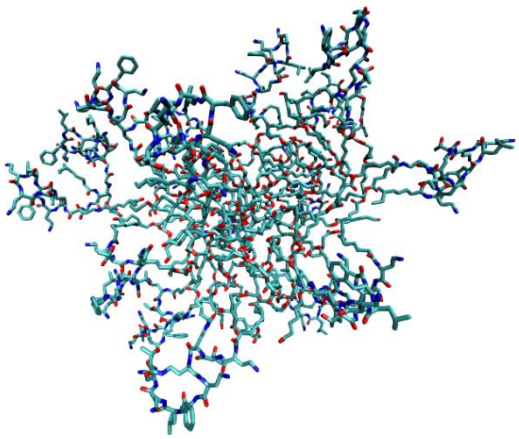

(B)

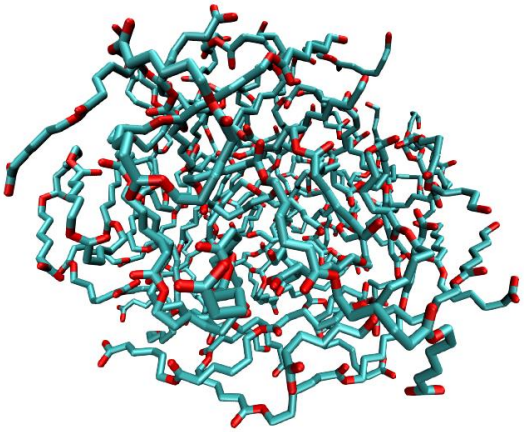

(C)

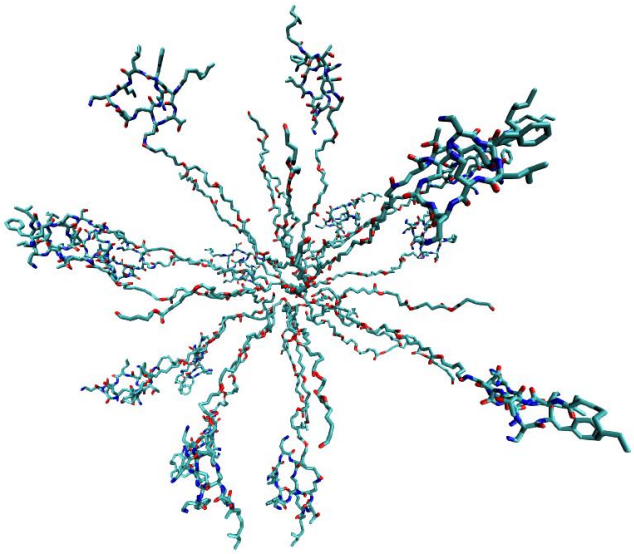

Figure 9- AMP (A) and control (B) micelles, after 20 ns simulation and the starting position (C) for the AMP micelle. Both micelles shape remained stable during the simulation. The control micelle starting structure used the same base as the one with AMP, but the peptide was removed.

Micelle stability

To understand the properties of the AMP bonded micelle, they were compared to the control micelle without AMP. Due to the lack of more similar micelle information for comparison, the structural information of software-made detergent micelles from Krüger & Kamerlin, 2017 (supplemental table S1) was used as a reference of normal micelle parameters.

The eccentricity of the micelles was evaluated from 17.5 ns to 20 ns. While the eccentricity fluctuates, the micelle with polymyxin B averages at 0.172 with a standard deviation of 0.026. When compared to simulations of the control micelle with an average of 0.169 with a standard deviation of 0.029 the bonded AMP appears to not drastically alter the eccentricity. However, the reference micelles have their eccentricity between 0.083±0.031 (α-DDM) and 0.153±0.045 (β-NG) which is lower than either PCL micelle, but the micelles appear to be stable even if they are not completely spherical.

The average effective micelle radius in the same interval is 32.14 Å for the micelle with polymyxin B, while the control micelle was a radius of 18.783 Å. The reference micelles have a minimum size of 24.73±0.39 Å (β-OM) and a maximum size of 34.71±0.41 Å (β-DDM), a range that includes the created micelles.

In the micelle with polymyxin B, the solvent accessible surface area (SASA) of the micelle hydrophobic (PHO) components is on average 6258.486 $Å^2$ and the hydrophilic (PHI) components is 19253.975 $Å^2$, which has a PHI/PHO ratio of 3.083. When the ratio is higher, it corresponds to a more thermodynamically favourable disposition of the micelle domains (Lebecque et al., 2016). However in this specific case some of the hydrophilic AMPs are not fully in contact with the core so it may not be wise to evaluate this micelle on this parameter the way the others are since the ratio doesn't correlate entirely to how much the hydrophilic domains shields the core. The control micelle has a SASA of 9270.661 $Å^2$ so the micelles AMPs cover 67.5085% of the surface area.

The hydrophobic residues appear to have contact with water but there is not hydration at the core. Despite the contact of PCL with water, there is no water inside the micelle.

The micelles appear to have the PCL molecules move within the core in such a manner that some chains appear to be entirely on the surface. This is most likely due to the extremely simplified conditions chosen for the micelle formation. In future works, the micelle stability would be taken into account, using PEG as a hydrophilic block for the chains without AMP or adding a more hydrophobic component to PCL to maximize the hydrophobic potential. It could be possible to attempt the simulations with alternative formulations of the peptides, such as an analogue with a lower charge to avoid repulsion. The choice of position used to bond the AMP with the PCL chain can be reviewed, to minimize the impact on the functionality.

Membrane model

As it is most frequent, this work was based on *E. coli* as a model-organism for the study of AMP membrane interactions. The membrane was created using CHARMM-GUI membrane builder to create a pdb file with the molecules distributes as intended in a bilayer.

For simplicity, the outer membrane external layer, was constituted of only LPS, since other lipids have low composition enough to omit (Rice & Wereszczynski, 2018; Wu et al., 2014). The inner leaflet of the outer membrane was composed of phosphatidylethanolamine (PE) and phosphatidylglycerol (PG), which are the two main classes of lipids of the inner membrane leaflet (Wu et al., 2014). The ratio between them is 3: 1, since PE constitutes 75% of the lipids in the inner leaflet and the other components are far less present (Wu et al., 2014). The charges of lipid A phosphate groups were neutralized with calcium and the remaining negative charges with sodium (Patel, Qi, & Im, 2017; Rice & Wereszczynski, 2018).

Due to the variety and size of LPS, lipid A without core or O-antigen was used as the simplest form rough LPS. The polymyxin B targets the phosphate groups in the lipid A, therefore both the simulation time required for their interaction

and the number of atoms in the system is reduced. Unfortunately, the software's limitation causes the LPS to not be placed correctly, likely due to the modularity of LPS construction being incompatible with the adjustments applied to the other membrane molecules, as the software's membrane visualization option, seen in figure 10, does not recognise the LPS atoms as a single molecule even though it recognizes the remaining molecules. The end result is overlapping lipid tails as the LPS are placed as rigid structures, instead of being adjusted like PE and PG were, as seen in figure 11.

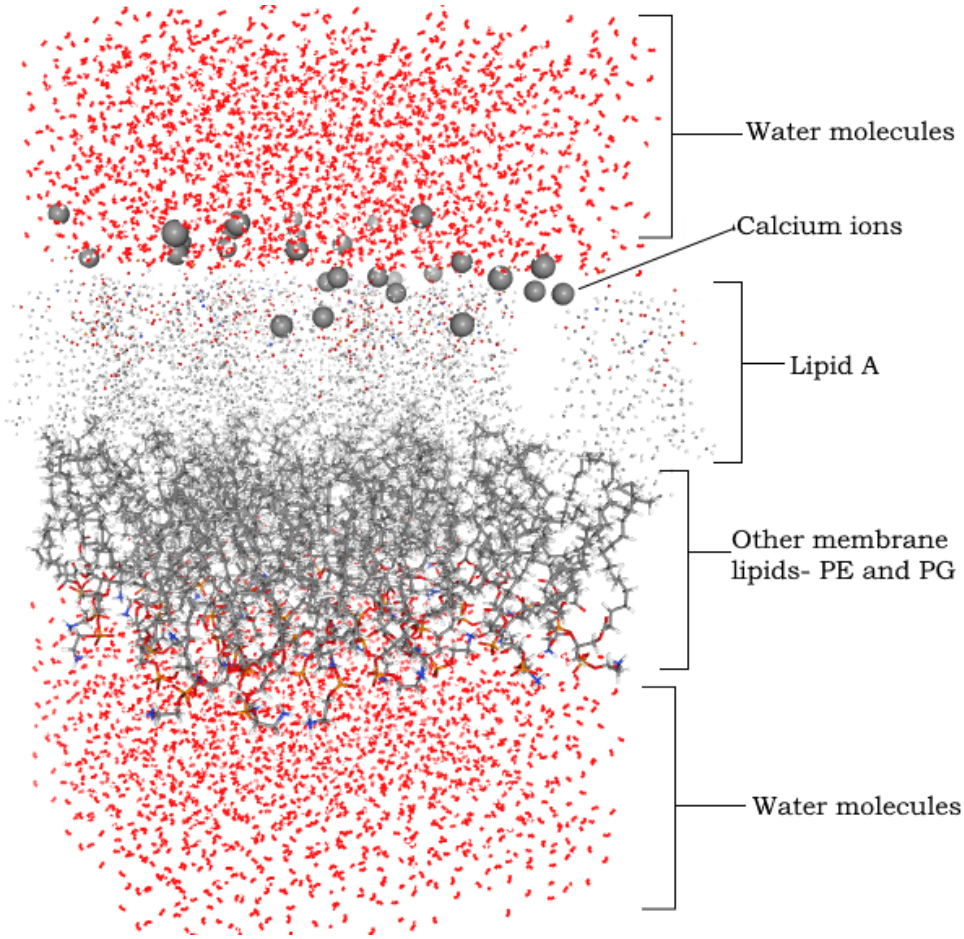

Figure 10- Visualization of the construction of the membrane in CHARMM-GUI, demonstrating the flaw of the micelle placement. LPS are shown as individual atoms; other membrane molecules are shown as full molecules. The red molecules are water and the large grey spheres are calcium ions.

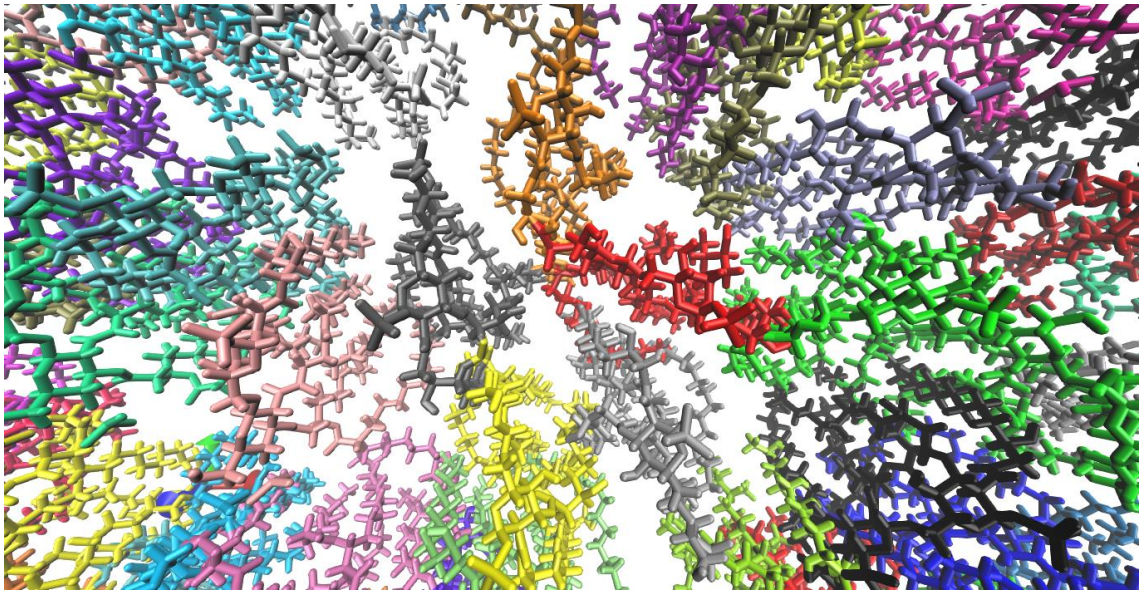

Figure 11- Close-up of lipid A molecules in the membrane, highlighting the overlaps of lipid tails. Each residue is shown in a different colour to add contrast.

However the overlap of LPS lipid tails during the structure creation led to the need for the membrane minimization to be more complex, using NAMD (Phillips et al., 2020) to restrict the structure so only the LPS lipid tails move, so the system can be properly equilibrated. This is done using the VMD (Humphrey, Dalke, & Schulten, 1996) scripting tool to attribute a beta value of 0 to the atoms that are intended to equilibrate, and to attribute a beta value of 1 to the atoms that are restrained, which can be seen in figure 12.

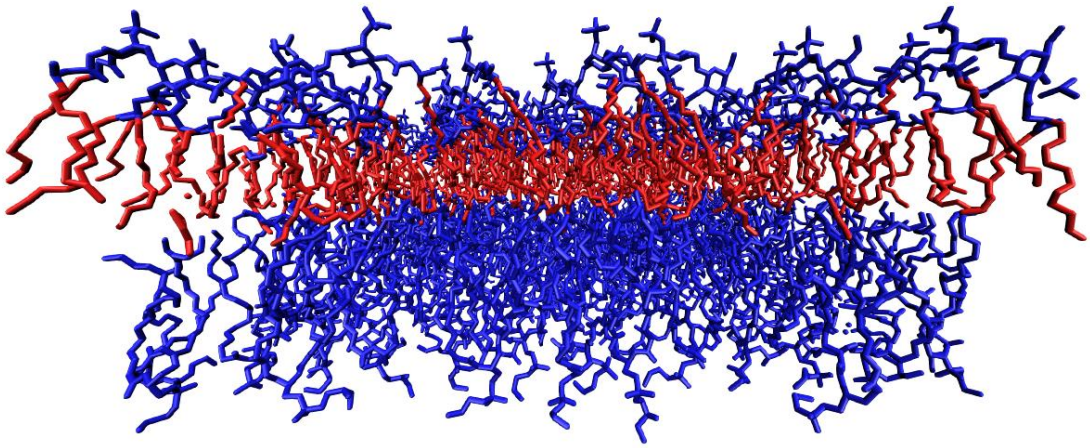

Figure 12- Membrane structure, where the atoms in red represent the unrestrained lipid tails of LPS, with a beta value of 0, and in blue the remaining

atoms, with a beta value of 1. Omitted in this image, water and ions also have a beta value of 1

In this step the CHARMM force field was used, as the force field that the input generator creates the parameters for by default. The equilibration of the membrane first started by restricting every atom except those in LPS lipid tails and lasted 1 nanosecond.

Then minimization continued for 20 ns without the restrictions on atoms followed by 10 ns more of simulation without the minimization.

For compatibility, to simulate the membrane with the AMP, both must be under the same force field.

Using AMBER's charmm2amber.py script, it is possible to substitute the atom and residue designations to AMBER's for both inner leaflet lipids. The main difference between CHARMM and AMBER lipid force field is the residue labelling, as in CHARMM every residue is an entire lipid molecule and in AMBER the molecule is split in smaller residues, as a form of modularity. However, lipid A is not supported in this script so the antechamber tool was used to create a mol2 file that includes the information for parameters. Calcium ions were also not covered in this script, but the search and replace function solved that oversight.

Other required modification of the file were the renumbering of lipid A residues, as all were set as residue 1, and the separation of molecules in the file with the indicator "TER", in accordance with PDB format. This was done with python code.

First, the file was opened with python to load the data in lists. Using the split() function on each line, the values of each column can be assigned to variables, which are then appended to a list for each. The residue numbers of lipid A were replaced, by using a counter that increases when the first atom of the molecule

is encountered. Using string formatting, the columns were rewritten in the pdb spacing and alignment format.

Before any of the first atoms either LPS or inner leaflet molecules, a "TER" indicator was written on the file. The atoms were specifically: HB6S of LPS and C12 of PA a residue common to both PG and PE, as part of AMBER lipids modularity.

Conclusions and Future Perspectives

This project, while not having fulfilled the proposed objectives within the available time, still accomplished useful results:
-A stable micelle with PCL and polymyxin B that is ready for testing;
-An AMBER-compatible equilibrated *E.coli* membrane model;
-Several snippets of python code for pdb editing, specifically reformatting files and renumbering and separating residues.

The results in this work are preliminary, setting a precedent for a new way to utilize antimicrobial peptides for medical purposes. Although this work is very conservative, to minimize the number of variables, further research would establish a better understanding that will allow designing an optimized micelle to be tested. This would allow *in vitro* testing to not have unproductive experiments.

The works elaborating on this one can take this base approach and incorporate the above referred stabilization mechanisms.

References

Almeida, B. C., Figueiredo, P., & Carvalho, A. T. P. (2019). Polycaprolactone Enzymatic Hydrolysis: A Mechanistic Study. *ACS Omega*, *4*(4), 6769–6774. https://doi.org/10.1021/acsomega.9b00345

Burley, S. K., Berman, H. M., Bhikadiya, C., Bi, C., Chen, L., Di Costanzo, L., … Ioannidis, Y. E. (2019). Protein Data Bank: The single global archive for 3D macromolecular structure data. *Nucleic Acids Research*, *47*(D1), D520–D528. https://doi.org/10.1093/nar/gky949

Case, D. A., Belfon, K., Ben-Shalom, I. Y., Brozell, S. R., Cerutti, D. S., T.E. Cheatham, I., … Kollman, P. A. (2020). Amber 2020. *University of California, San Francisco*.

Chapman, J., Ismail, A. E., & Dinu, C. Z. (2018). Industrial applications of enzymes: Recent advances, techniques, and outlooks. *Catalysts*, *8*(6), 20–29. https://doi.org/10.3390/catal8060238

Cheng, X., Jo, S., Lee, H. S., Klauda, J. B., & Im, W. (2013). CHARMM-GUI Micelle Builder for Pure/Mixed Micelle and Protein/Micelle Complex Systems. *Journal of Chemical Information and Modeling*, *53*(8), 2171–2180. https://doi.org/10.1021/ci4002684

Connolly, M. L. (1983). Analytical molecular surface calculation. *Journal of Applied Crystallography*, *16*(5), 548–558. https://doi.org/10.1107/s0021889883010985

Dash, T. K., & Konkimalla, V. B. (2012). Poly-ε-caprolactone based formulations for drug delivery and tissue engineering: A review. *Journal of Controlled Release*, *158*(1), 15–33. https://doi.org/10.1016/j.jconrel.2011.09.064

Debye, P., Anacker, E., & Anacker', E. W. (1950). Micelle shape from dissymetry measurements. J. Phys. Chem., 644–655.

Dickson, C. J., Madej, B. D., Skjevik, Å. a., Betz, R. M., Teigen, K., Gould, I. R., & Walker, R. C. (2014). Lipid14: The Amber Lipid Force Field. *Journal of Chemical Theory and Computation*, *10*(2), 865–879. https://doi.org/dx.doi.org/10.1021/ct4010307

Durrant, J. D., & Mccammon, J. A. (2011). Molecular dynamics simulations and drug discovery. *BMC Biology*. Retrieved from http://www.biomedcentral.com/1741-7007/9/71

Engel, E., & Dreizler, R. M. (n.d.). *Density Functional Theory*.

Faramarzi, S., Bonnett, B., Scaggs, C. A., Ho, A., Grodi, D., Harvey, E., … Virginia, W. (2017). Molecular Dynamics Simulations as a Tool for Accurate Determination of Surfactant Micelle Properties. https://doi.org/10.1021/acs.langmuir.7b02666

French, S., Farha, M., Ellis, M. J., Sameer, Z., Côté, J. P., Cotroneo, N., … Brown, E. D. (2020). Potentiation of Antibiotics against Gram-Negative Bacteria by Polymyxin B Analogue SPR741 from Unique Perturbation of the Outer Membrane. *ACS Infectious Diseases*, *6*(6), 1405–1412. https://doi.org/10.1021/acsinfecdis.9b00159

Gerrit Groenhof. (2013). *Introduction to QM/MM Simulations*. *Methods Mol Biol* (Vol. 924). https://doi.org/10.1007/978-1-62703-017-5

Goodsell, D. S., Zardecki, C., Di Costanzo, L., Duarte, J. M., Hudson, B. P., Persikova, I., … Burley, S. K. (2020). RCSB Protein Data Bank: Enabling biomedical research and drug discovery. *Protein Science*, *29*(1), 52–65. https://doi.org/10.1002/pro.3730

Goswami, A., & Van Lanen, S. G. (2015). Enzymatic strategies and biocatalysts for amide bond formation: Tricks of the trade outside of the ribosome. *Molecular BioSystems*, *11*(2), 338–353. https://doi.org/10.1039/c4mb00627e

Groenhof, G. (2013). Introduction to QM/MM Simulations. In *Biomolecular Simulations: Methods and Protocols, Methods in Molecular Biology* (Vol. 924, pp. 43–66). https://doi.org/10.1007/978-1-62703-017-5

Grossen, P., Witzigmann, D., Sieber, S., & Huwyler, J. (2017). PEG-PCL-based nanomedicines : A biodegradable drug delivery system and its application. *Journal of Controlled Release*, *260*(May), 46–60. https://doi.org/10.1016/j.jconrel.2017.05.028

Hancock, R. E. W. (2000). Expert Opinion on Investigational Drugs- Cationic antimicrobial peptides : towards clinical applications, 1723–1729.

Harris, C. R., Millman, K. J., van der Walt, S. J., Gommers, R., Virtanen, P., Cournapeau, D., … Oliphant, T. E. (2020). Array programming with NumPy. *Nature*, *585*(7825), 357–362. https://doi.org/10.1038/s41586-020-2649-2

Harrison, J. A., Schall, J. D., Maskey, S., Mikulski, P. T., Knippenberg, M. T., Morrow, B. H., … Morrow, B. H. (2018). Review of force fields and intermolecular potentials used in atomistic computational materials research, *031104*. https://doi.org/10.1063/1.5020808

Hollingsworth, S. A., & Dror, R. O. (2018). Molecular Dynamics Simulation for All. *Neuron*, *99*(6), 1129–1143. https://doi.org/10.1016/j.neuron.2018.08.011

Humphrey, W., Dalke, A., & Schulten, K. (1996). VMD - Visual Molecular Dynamics. *Journal of Molecular Graphics*, *14*, 33–38.

Hunter, J. D. (2007). Matplotlib: A 2D graphics environment. *Computing in Science and Engineering*, *9*(3), 90–95. https://doi.org/10.1109/MCSE.2007.55

Javanainen, M., & Martinez-seara, H. (2016). Efficient preparation and analysis of membrane and membrane protein systems. *Biochimica et Biophysica Acta- Biomembranes*, *1858*(10), 2468–2482. https://doi.org/10.1016/j.bbamem.2016.02.036

Javia, A., Amrutiya, J., Lalani, R., Patel, V., Bhatt, P., & Misra, A. (2018). Antimicrobial peptide delivery: An emerging therapeutic for the treatment of burn and wounds. *Therapeutic Delivery*, *9*(5), 375–386. https://doi.org/10.4155/tde-2017-0061

Jiang, Y., & Loos, K. (2016). Enzymatic synthesis of biobased polyesters and polyamides. *Polymers*, *8*(7). https://doi.org/10.3390/polym8070243

Jo, S., Kim, T., Iyer, V. G., & Im, W. (2008). CHARMM-GUI: A web-based graphical user interface for CHARMM. *Journal of Computational Chemistry*, *29*(11), 1859–1865. https://doi.org/https://doi.org/10.1002/jcc.20945

Kedar, U., Phutane, P., Shidhaye, S., & Kadam, V. (2010). Advances in polymeric micelles for drug delivery and tumor targeting. *Nanomedicine: Nanotechnology, Biology, and Medicine*, *6*(6), 714–729. https://doi.org/10.1016/j.nano.2010.05.005

Kirk, O., Borchert, T. V., & Fuglsang, C. C. (2002). Industrial enzyme applications. *Current Opinion in Biotechnology*, *13*(4), 345–351. https://doi.org/10.1016/S0958-1669(02)00328-2

Krüger, D. M., & Kamerlin, S. C. L. (2017). Micelle Maker: An Online Tool for Generating Equilibrated Micelles as Direct Input for Molecular Dynamics Simulations. *ACS Omega*, *2*(8), 4524–4530. https://doi.org/10.1021/acsomega.7b00820

Lam, C. X. F., Hutmacher, D. W., Schantz, J. T., Woodruff, M. A., & Teoh, S. H. (2009). Evaluation of polycaprolactone scaffold degradation for 6 months in vitro and in vivo. *Journal of Biomedical Materials Research. Part A*, *90*(3), 906–919. https://doi.org/10.1002/jbm.a.32052

Langham, A., & Kaznessis, Y. N. (2010). Molecular Simulations of Antimicrobial Peptides. *Methods Mol Biol*, (618), 267–285. https://doi.org/10.1007/978-1-60761-594-1_17

Lebecque, S., Crowet, J. M., Nasir, M. N., Deleu, M., & Lins, L. (2016). Molecular Dynamics Study of Micelles Properties According to their Size. *Journal of Molecular Graphics and Modelling*. https://doi.org/10.1016/j.jmgm.2016.12.007

Lei, J., Sun, L. C., Huang, S., Zhu, C., Li, P., He, J., … He, Q. (2019). The antimicrobial peptides and their potential clinical applications. *American Journal of Translational Research*, *11*(7), 3919–3931.

Lenhard, J. R., Bulman, Z. P., Tsuji, B. T., & Kaye, K. S. (2019). Shifting gears: The future of polymyxin antibiotics. *Antibiotics*, *8*(2), 1–13. https://doi.org/10.3390/antibiotics8020042

Lepak, A. J., Wang, W., & Andes, D. R. (2020). Pharmacodynamic Evaluation of MRX-8, a Novel Polymyxin, in the Neutropenic Mouse Thigh and Lung Infection Models against Gram-Negative Pathogens. *Antimicrobial Agents and Chemotherapy*, *64*(11), 1–11. https://doi.org/10.1128/AAC.01517-20

Levine, I. N. (2000). *Quantum Chemistry - Ira Levine - 5th edition* (5th ed.).

Liechty, W. B., Kryscio, D. R., Slaughter, B. V., & Peppas, N. A. (2010). Polymers for drug delivery systems. *Annual Review of Chemical and Biomolecular Engineering*, *1*, 149–173. https://doi.org/10.1146/annurev-chembioeng-073009-100847

Lu, Y., Zhang, E., Yang, J., & Cao, Z. (2018). Strategies to improve micelle stability for drug delivery. *Nano Res*, (11), 4985–4998. https://doi.org/doi:10.1007/s12274-018-2152-3

Magana, M., Pushpanathan, M., Santos, A. L., Leanse, L., Fernandez, M., Ioannidis, A., … Tegos, G. P. (2020). The value of antimicrobial peptides in the age of resistance. *The Lancet Infectious Diseases*, *20*(9), e216–e230. https://doi.org/10.1016/S1473-3099(20)30327-3

Maier, J. A., Martinez, C., Kasavajhala, K., Wickstrom, L., Hauser, K., & Simmerling, C. (2015). ff14SB : Improving the accuracy of protein side chain and backbone parameters from ff99SB.

Mandal, P., & Shunmugam, R. (2020). Polycaprolactone: a biodegradable polymer with its application in the field of self-assembly study. *Journal of Macromolecular Science, Part A: Pure and Applied Chemistry*, *58*(2), 111–129. https://doi.org/10.1080/10601325.2020.1831392

Mardirossian, N., & Head-gordon, M. (2017). Thirty years of density functional theory in computational chemistry : an overview and extensive assessment of 200 density functionals, *8976*. https://doi.org/10.1080/00268976.2017.1333644

Marggraf, M. B., Panteleev, P. V., Emelianova, A. A., Sorokin, M. I., Bolosov, I. A., Buzdin, A. A., … Ovchinnikova, T. V. (2018). Cytotoxic potential of the novel horseshoe crab peptide polyphemusin III. *Marine Drugs*, *16*(12), 1–19. https://doi.org/10.3390/md16120466

Martin-Serrano, Á., Gómez, R., Ortega, P., & Mata, F. J. D. La. (2019). Nanosystems as vehicles for the delivery of antimicrobial peptides (Amps). *Pharmaceutics*, *11*(9), 1–24. https://doi.org/10.3390/pharmaceutics11090448

Martinez-Diaz, S., Garcia-Giralt, N., Lebourg, M., Gómez-Tejedor, J. A., Vila, G., Caceres, E., … Monllau, J. C. (2010). In Vivo Evaluation of 3-Dimensional Polycaprolactone Scaffolds for Cartilage Repair in Rabbits. *American Journal of Sports Medicine*, *38*(3), 509–519. https://doi.org/10.1177/0363546509352448

McKinney, W. (2010). Data Structures for Statistical Computing in Python. *Proceedings of the 9th Python in Science Conference*, *1*(Scipy), 56–61. https://doi.org/10.25080/majora-92bf1922-00a

Melani, N. B., Tambourgi, E. B., & Silveira, E. (2020). Lipases: From Production to Applications. *Separation and Purification Reviews*, *49*(2), 143–158. https://doi.org/10.1080/15422119.2018.1564328

Mendieta-moreno, J. I., & Marcos-alcalde, I. (2015). *Molecular Mechanics Method for the Dynamical Study of Reactions in Biomolecules*. *Combined Quantum Mechanical and Molecular Mechanical Modelling of Biomolecular Interactions* (1st ed., Vol. 100). Elsevier Inc. https://doi.org/10.1016/bs.apcsb.2015.06.003

Millman, K. J., & Aivazis, M. (2011). Python for scientists and engineers. *Computing in Science and Engineering*, *13*(2), 9–12. https://doi.org/10.1109/MCSE.2011.36

Navvabi, A., Razzaghi, M., Fernandes, P., Karami, L., & Homaei, A. (2018). Novel lipases discovery specifically from marine organisms for industrial production and practical applications. *Process Biochemistry*, *70*(March), 61–70. https://doi.org/10.1016/j.procbio.2018.04.018

Neese, F. (2009). Density functional theory, 443–453. https://doi.org/10.1007/s11120-009-9404-8

Nordström, R., & Malmsten, M. (2017). *Delivery systems for antimicrobial peptides*. *Advances in Colloid and Interface Science* (Vol. 242). Elsevier B.V. https://doi.org/10.1016/j.cis.2017.01.005

Owen, S. C., Chan, D. P. Y., & Shoichet, M. S. (2012). Polymeric micelle stability. *Nano Today*, *7*(1), 53–65. https://doi.org/10.1016/j.nantod.2012.01.002

Patel, D. S., Qi, Y., & Im, W. (2017). Modeling and simulation of bacterial outer membranes and interactions with membrane proteins. *Current Opinion in Structural Biology*. Elsevier Ltd. https://doi.org/10.1016/j.sbi.2017.01.003

Phillips, J. C., Hardy, D. J., Maia, J. D. C., Stone, J. E., Ribeiro, J. V., Bernardi, R. C., … Tajkhorshid, E. (2020). Scalable molecular dynamics on CPU and GPU architectures with NAMD. *Journal of Chemical Physics*, *153*(4). https://doi.org/10.1063/5.0014475

Phillips, J. N. (1954). The energetics of micelle formation. Transactions of the Faraday Society, 561–569.

Powers, J. S., Martin, M. M., Goosney, D. L., & Hancock, R. E. W. (2006). The Antimicrobial Peptide Polyphemusin Localizes to the Cytoplasm of Escherichia coli following Treatment. *ANTIMICROBIAL AGENTS AND CHEMOTHERAPY*, *50*(4), 1522–1524. https://doi.org/10.1128/AAC.50.4.1522

Powers, J. S., Rozek, A., & Hancock, R. E. W. (2004). Structure-activity relationships for the β-hairpin cationic antimicrobial peptide polyphemusin I. *Biochimica et Biophysica Acta - Proteins and Proteomics*, *1698*(2), 239–250. https://doi.org/10.1016/j.bbapap.2003.12.009

Raman, A. S., Pajak, J., & Chiew, Y. C. (2018). Interaction of PCL based self-assembled nano-polymeric micelles with model lipid bilayers using coarse-grained molecular dynamics simulations. *Chemical Physics Letters*, *712*(August), 1–6. https://doi.org/10.1016/j.cplett.2018.09.049

Rice, A., & Wereszczynski, J. (2018). Atomistic Scale Effects of Lipopolysaccharide Modifications on Bacterial Outer Membrane Defenses. *Biophysj*, *114*(6), 1389–1399. https://doi.org/10.1016/j.bpj.2018.02.006

Rose, F., Heuer, K. U., Sibelius, U., Hombach-Klonisch, S., Kiss, L., Seeger, W., & Grimminger, F. (2000). Targeting lipopolysaccharides by the nontoxic polymyxin B nonapeptide sensitizes resistant Escherichia coli to the bactericidal effect of human neutrophils. *Journal of Infectious Diseases*, *182*(1), 191–199. https://doi.org/10.1086/315669

Salomon-ferrer, R., Case, D. A., & Walker, R. C. (2012). An overview of the Amber biomolecular simulation package, *00*(February), 1–13. https://doi.org/10.1002/wcms.1121

Sandreschi, S., Piras, A. M., Batoni, G., & Chiellini, F. (2016). Perspectives on polymeric nanostructures for the therapeutic application of antimicrobial peptides. *Nanomedicine*, *11*(13), 1729–1744. https://doi.org/10.2217/nnm-2016-0057

Seidi, F., Jenjob, R., & Crespy, D. (2018). Designing Smart Polymer Conjugates for Controlled Release of Payloads. *Chemical Reviews*, *118*(7), 3965–4036. https://doi.org/10.1021/acs.chemrev.8b00006

Sharma, S., Kumar, P., & Chandra, R. (2019). Introduction to molecular dynamics. *Molecular Dynamics Simulation of Nanocomposites Using BIOVIA Materials Studio, Lammps and Gromacs*, *23*, 1–38. https://doi.org/10.1016/B978-0-12-816954-4.00001-2

Shuai, X., Ai, H., Nasongkla, N., Kim, S., & Gao, J. (2004). Micellar carriers based on block copolymers of poly(ε-caprolactone) and poly(ethylene glycol) for doxorubicin delivery. *Journal of Controlled Release*, *98*(3), 415–426. https://doi.org/10.1016/j.jconrel.2004.06.003

Speranzini, V., Rotili, D., Ciossani, G., Pilotto, S., Marrocco, B., Forgione, M., … Mattevi, A. (2016). Polymyxins and quinazolines are LSD1/KDM1A inhibitors with unusual structural features. *Science Advances*, *2*(9), 2–10. https://doi.org/10.1126/sciadv.1601017

Sprenger, K. G., Jaeger, V. W., & Pfaendtner, J. (2015). The general AMBER force field (GAFF) can accurately predict thermodynamic and transport properties of many ionic liquids. *Journal of Physical Chemistry B*, *119*(18), 5882–5895. https://doi.org/10.1021/acs.jpcb.5b00689

Stenberg, S., & Stenqvist, B. (2020). An Exact Ewald Summation Method in Theory and

Practice. *Journal of Physical Chemistry A*, *124*(19), 3943–3946. https://doi.org/10.1021/acs.jpca.0c01684

Sun, H., Hong, Y., Xi, Y., Zou, Y., Gao, J., & Du, J. (2018). Synthesis, Self-Assembly, and Biomedical Applications of Antimicrobial Peptide-Polymer Conjugates. *Biomacromolecules*, *19*(6), 1701–1720. review-article. https://doi.org/10.1021/acs.biomac.8b00208

Tanford, C. (1972). Micelle Shape and Size'. J. Phys. Chem, 76(21), 3020–3024.

Tanford, C. (1974). Theory of Micelle Formation in Aqueous Solutions. J. Phys. Chem., 2469–2479.

Thiel, W. (2009). QM / MM Methodology : Fundamentals , Scope , and Limitations. *Multiscale Simulation Methods in Molecular Sciences*, *42*, 203–214.

Vaara, M. (2019). Polymyxins and their potential next generation as therapeutic antibiotics. *Frontiers in Microbiology*, *10*(JULY), 1–6. https://doi.org/10.3389/fmicb.2019.01689

Vanommeslaeghe, K., Hatcher, E., Acharya, C., Kundu, S., Zhong, S., Shim, J., … Mackerell jr, A. D. (2009). CHARMM General Force Field: A Force Field for Drug-Like Molecules Compatible with the CHARMM All-Atom Additive Biological Force Fields. *Journal of Computational Chemistry*, *3*(Jornal of Computional Chemistry), 174–182. https://doi.org/10.1002/jcc.21367

Velkov, T., Thompson, P. E., Nation, R. L., & Li, J. (2010). Structure-activity relationships of polymyxin antibiotics. *Journal of Medicinal Chemistry*, *53*(5), 1898–1916. https://doi.org/10.1021/jm900999h

Wang, J., Wolf, R. M., Caldwell, J. W., Kollman, P. A., & Case, D. A. (2004). Development and testing of a general Amber force field. *Journal of Computational Chemistry*, *25*(9), 1157–1174. https://doi.org/10.1002/jcc.20035

Wang, Y., Fass, J., & Chodera, J. D. (2020). End-to-End Differentiable Molecular Mechanics Force Field Construction.

Weiser, J., Shenkin, P. S., & Still, W. C. (1998). Approximate Atomic Surfaces from Linear Combinations of Pairwise, *20*(2), 217–230.

Wu, E. L., Fleming, P. J., Yeom, M. S., Widmalm, G., Klauda, J. B., Fleming, K. G., & Im, W. (2014). E. coli outer membrane and interactions with OmpLA. *Biophysical Journal*, *106*(11), 2493–2502. https://doi.org/10.1016/j.bpj.2014.04.024

Yurkova, M. S., Zenin, V. A., Sadykhov, E. G., & Fedorov, A. N. (2020). Dimerization of Antimicrobial Peptide Polyphemusin I into One Polypeptide Chain: Theoretical and Practical Consequences. *Applied Biochemistry and Microbiology*, *56*(9), 893–897. https://doi.org/10.1134/S0003683820090100

Zhu, M., Liu, P., & Niu, Z. W. (2017). A perspective on general direction and challenges facing antimicrobial peptides. *Chinese Chemical Letters*, *28*(4), 703–708. https://doi.org/10.1016/j.cclet.2016.10.001

ANEX I

List of software

AMBER

A compilation of programs for molecular dynamics focused in biomolecules. The name also applies to the empirical force fields implemented for said programs.(Case et al, 2020)

Leap- program to create and modify systems for molecular dynamics, using molecules in input files such pdb or mol2, and building the parameter and topology files. (Case et al, 2020)

Antechamber - program that allows calculate force field of small molecules that aren't included in the force field, such as drugs and modified amino acids. (Case et al, 2020)

Sander- a tool that can equilibrate the system and run molecular dynamics. (Case et al, 2020)

Pmemd- an improvement of sander, allowing faster simulations and the support for GPU (graphic processing unit) acceleration. (Case et al, 2020)

Cpptraj- main program for analyzing dynamic output files, such as calculating values of bonds or angles, measure fluctuation and analyze hydrogen bonds. (Case et al, 2020)

CHARMM-GUI online input generator

Web-based plataform to generate complex systems for molecular dynamics, that supports multiple force fields and with several application such as the construction of large structures including membranes and micelles (S. Jo, T. Kim, V.G. Iyer, and W. Im, 2008).

NAMD

A cross-platform molecular simulation software that uses scalable parallel processing for high performance simulations (Phillips et al., 2020). NAMD supports multiple force fields, including AMBER and CHARMM(Phillips et al., 2020).

VMD(Visual Molecular Dynamics)

Visualization software for displaying, animating and analysing large bio molecular systems. Supports various file types, such as pdb, although Windows version requires AMBER output to be converted with cpptraj(Humphrey, W., Dalke, A. and Schulten, K, 1996)

ANEX II

Python Code

Part 1

Coordinate convertion code, adapted from https://stackoverflow.com/questions/57794357 (visited on 15th of January of 2021)

```
def Cartesian2Spherical(p):
        x,y,z = p
        r = np.sqrt(x*x+y*y+z*z)
        phi = np.arctan2(y,x)  # Inclination
        theta = np.arccos(z/r)  # Azimuth
        q = np.array([r,theta,phi])
        return q

def Spherical2Cartesian(q):
        r,theta,phi = q
        SinTheta = np.sin(theta)
        CosTheta = np.cos(theta)
        SinPhi = np.sin(phi)
        CosPhi = np.cos(phi)
        rSinTheta = r*SinTheta
        x = rSinTheta*CosPhi
        y = rSinTheta*SinPhi
        z = r*CosTheta
        p  = np.array([x,y,z])
        return p
```

Part 2

Spherical point generator, adapted from https://stackoverflow.com/questions/9600801 (visited on 24th of February 2021)

```
def fibonacci_sphere(samples):
        points = []
        phi = math.pi * (3. - math.sqrt(5.))  # golden angle in
radians
        for i in range(samples):
                y = 1 - (i / float(samples - 1)) * 2  # y goes
from 1 to -1
                radius = math.sqrt(1 - y * y)  # radius at y
                theta = phi * i  # golden angle increment
```

```
10                  x = math.cos(theta) * radius
11                  z = math.sin(theta) * radius
                    points.append((x, y, z))
            return points
```

Part 3

Code to Renumber the residues, write them to file with the pdb format and add a "TER" indicator between residues. Original.

```
 1 output = open ("Membrane_renumbered.pdb", 'w')
 2 space = ' '
 3 newline= '\n'
 4 recordtype_list = []
 5 name_list = []
 6 number_list = []
 7 resname_list = []
 8 resid_list = []
 9 X_list = []
10 Y_list = []
11 Z_list = []
12 t_factor_list = []
13 occupancy_list = []
14 chain_list = []
15 guide_list = []
16 n=0
17 LPS = 'LPSA'
18 firstatom_LPS = 'HB6S'
19 firstatom_PA = 'C12  PA'
20
21 with open('Membrane_reference.pdb', 'r') as f:
22         for line in f:
23                 line_data = line.split()
24                 if "ATOM" in line_data:
25                         recordtype, number, name, resname, resid,
   X, Y, Z, occupancy, t_factor, chain = line_data
26                         guide_list.append(recordtype)
27                         recordtype_list.append(recordtype)
28                         number_list.append(number)
29                         name_list.append(name)
30                         resname_list.append(resname)
31                         X_list.append(float(X))
32                         Y_list.append(float(Y))
33                         Z_list.append(float(Z))
34                         t_factor_list.append(float(t_factor))
35                         occupancy_list.append(float(occupancy))
36                         chain_list.append(chain)
```

```
                        if LPS not in line_data:
                                resid_list.append(resid)
                        elif LPS in line_data:
                                if firstatom_LPS in line_data:
                                        guide_list.append('TER')
                                        n+=1
                                resid_list.append(n)
                elif "TER" in line_data:
                        guide_list.append('TER')

number_list = [str(num) for num in number_list]
resid_list = [str(res) for res in resid_list]

for i in range(len(recordtype_list)):
        if guide_list == 'TER':
                output.writelines('TER\n')
        else:
                output.writelines(f"{recordtype_list[i] :
<4}{number_list[i] : >7s}{space : >1}{name_list[i] : <4}{space :
>1}{resname_list[i] : <4}{resid_list[i] : >5s}{X_list[i] :
>12.3f}{Y_list[i] : >8.3f}{Z_list[i] : >8.3f}{t_factor_list[i] :
>6.2f}{occupancy_list[i] : >6.2f}{chain_list[i] : >10}{newline :
>1}")
output.close()

output = open ("Membrane_AMBER_TER_resname_test.pdb", 'w')

with open('Membrane_resnumbered.pdb', 'r') as f:
        for line in f:
                if "ATOM" in line:
                        if firstatom_LPS in line or firstatom_PA
in line:
                                output.writelines('TER\n')
                                output.writelines(line)
                        else:
                                output.writelines(line)
output.close()
```